SEISMIC ATTRIBUTES FOR RESERVOIR CHARACTERIZATION

IN DEEPWATER SETTINGS – GUAJIRA BASIN

OFFSHORE COLOMBIA

by

CLAUDIA ALEXANDRA RUBIO ZAPATA

ANDREW M. GOODLIFFE, COMMITTEE CHAIR
DELORES M. ROBINSON
BO ZHANG
JUAN C. LLINAS

A THESIS

Submitted in partial fulfillment of the requirements
for the degree of Master of Science
in the Department of Geological Sciences
in the Graduate School of
The University of Alabama

TUSCALOOSA, ALABAMA

2017

ABSTRACT

The uncertainties associated with reservoir identification during the exploration process are reduced through the use of methods including seismic attributes and inversion. These techniques provide interpreters with a powerful tool to enhance subsurface information, resulting in more accurate geologic models for play and prospect definition. Gas was discovered in a well drilled in 2014, confirming the hydrocarbon potential in the Guajira offshore basin. Given the high amplitude of target horizons and correlations with onshore rock exposures, it was initially interpreted as a carbonate hosted reservoir. Instead, the gas was hosted in an Eocene/Oligocene siliciclastic reservoir. After this discovery and the integration of the results into the regional framework, a search was made for an effective approach to avoid seismic misinterpretations related to lithological identification. This study used the reservoir petrophysical properties, to characterize the turbidite deposits using seismic attribute analysis and inversion, calibrating the well data with the seismic expression of 1,500 km^2 of reflection data (pre-stack time migration). A chronostratigraphic marker horizon, used to define the limits of extensional sedimentation undeformed by Late Miocene–Pliocene subduction (Mantilla et al., 2013), was the basis of this assessment. This included geometry and distribution, as well as seismic response and relations between seismic facies, seismic attributes, and petrophysical properties. The seismic methods applied in this study allowed the extension of borehole reservoir properties, specifically acoustic impedance, beyond the well into the seismic cube, even in the presence of a highly laminated siliciclastic reservoir. The resulting workflow is a tool that can be

used to reduce the time taken for reservoir mapping and modeling, providing an easier routine to update subsurface models for future drilling and development plans, and to reduce interpretation uncertainty.

LIST OF ABBREVIATIONS AND SYMBOLS

3-D	Three dimensional
CAL	Caliper well log
GR	Gamma Ray well log
DST	Drill Stem Test
DTCO	Compressional sonic well log
DTSM	Shear sonic well log
FMI	Fullbore Formation Microimager
MD	Measured depth
MDT	Modular Formation Dynamics Tester
MMSCFGD	Million standard cubic feet of gas per day
NMR	Nuclear Magnetic Resonance
PSTM	Pre-Stack Time Migration
RAI	Relative Acoustic Impedance
RES	Resistivity well log
RHOZ	Standard Resolution Formation Density well log
RT	True Resistivity well log
RXO	Flushed Zone Resistivity well log
SP	Spontaneous Potential well log
TNPH	Thermal Neutron Porosity well log

TWT	Two-way travel time
TVD	True vertical depth
UBI	Ultrasonic Borehole Imager

ACKNOWLEDGMENTS

My deepest thanks to my advisor and committee chair, Dr. Goodliffe, for his guidance through my graduate experience, encouraging me to be a better researcher. His friendliness, availability, and helpfulness were invaluable and worthy of admiration. Special thanks to my committee members, Drs. Robinson, Zhang and Llinas for all the support they gave me through this process. Their suggestions and substantial feedback provided quality and consistency to my project.

My gratitude to Ecopetrol S.A. for the data provided and the financial support towards the completion of my graduate studies at The University of Alabama. The North Caribbean Exploration Team, led by Victor Ramirez, are deeply thanked for their friendship and priceless support. You all trusted in me more than I trusted in myself.

Beth Partlow, Karen Linville, and the faculty and staff at the Department of Geological Sciences are truly thanked for their kind guidance and assistance, making life easier as a graduate student.

To my closest friends and family, you lifted me up when I needed you most. I am grateful for each day I shared with my husband and my son during this journey. Your love, faith and patience inspire my life. Mom, dad, brother . . . I am everything I am because of you; this is for you!!

CONTENTS

LIST OF TABLES

LIST OF FIGURES

1. INTRODUCTION

Subduction of the Caribbean and South American plates subduction began in Late Jurassic time (148 Ma; Pindell and Kennan, 2009). The Caribbean Plate originated as the proto-Caribbean seaway, which formed as South and North America moved apart (Figure 1a). By Late Cretaceous time, the Caribbean region was moving northward, the proto-Caribbean seaway was spreading, and the Caribbean Plate was in dextral motion relative to the northern Andes. Terrane migration occurred eastward by transpression at the northern and southern margins of the Caribbean Plate (Figure 1b). During Eocene time, a change in direction of motion was observed, the region drifted from west to east, incorporating Nicaragua onto the Caribbean plate; the southern part of the Panama Arc was accreted to the South American Plate (Figure 1c; Pindell and Kennan, 2009). By Miocene time, west to east migration continued and convergence in the region initiated development of the South Caribbean foldbelt. The Panama Arc reached the western Cordillera and started to move in a northwest direction (Figure 1d). The present-day configuration (Figure 1e) displays the main tectonic features of the Caribbean (Pindell and Kennan, 2009).

The Guajira Basin is located at the northern end of the South American plate (Figure 2). It is bounded to the north and northwest by the South Caribbean Deformed Belt (SCDB). The Oca fault bounds the basin to the south and the political boundary defines the eastern limit of the Colombian portion of the basin.

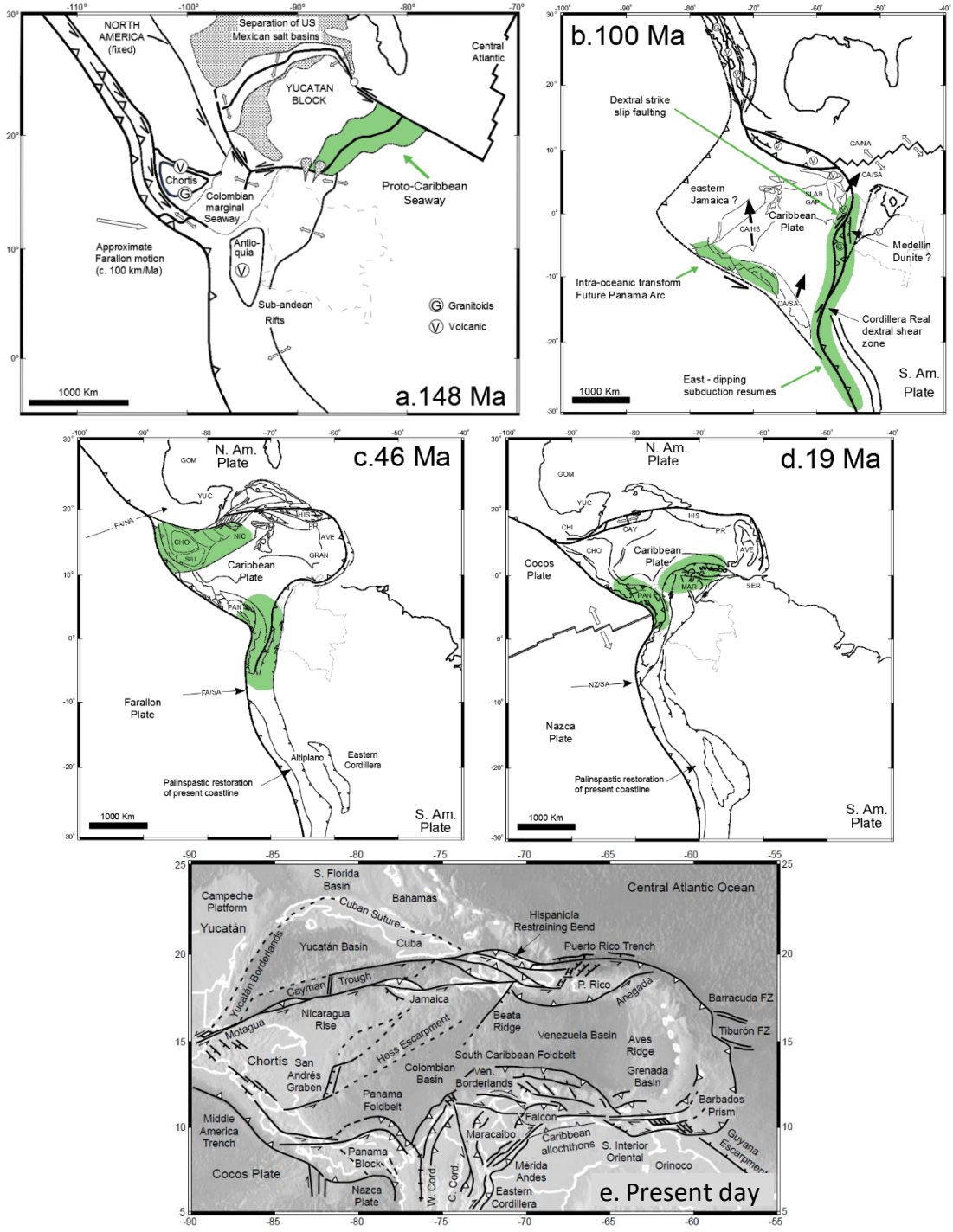

Figure 1. Caribbean region tectonic evolution from 148 Ma to present day. Events described above are highlighted in green (modified from Pindell and Kennan, 2009).

With an area close to 30,000 km^2 and approximately 30 exploratory wells located onshore and in shallow waters offshore (<80 m), the Guajira Basin is considered a frontier basin given the scarce knowledge provided by exploration that is still in its early stages. The gravity isostatic anomaly map (Ceron, 2008; Figure 3) shows the local tectonic features that controlled sedimentation. The Tayrona and Rancherias depressions are the main depocenters for Tertiary sediments. These are separated by the Carpintero high, which is an offshore extension of the Cosinas range (Figures 3 and 4) where Jurassic and Cretaceous rocks have been described as potential petroleum source rocks (Ramirez, 2007).

Ramirez (2007) summarized the stratigraphic studies that defined the nomenclature for the Guajira Basin, correlating outcrop data to well information (Figure 4). Tertiary lithostratigraphic units, deposited in unconformable contact over an igneous and metamorphic basement, were described by De Porta (1974), as follows:

Macarao Formation: This unit was defined by Rollins (1965) as a sequence of slightly carbonaceous clay interbedded with micaceous sandstone with glauconite (140 m), overlain by a massive and fossiliferous limestone (90 m). The presence of *Venericardia* mollusks defined the age as post-Campanian to pre-Oligocene. The formation is separated from the Siamana Formation by an angular unconformity. The type locality is 250 m thick, located 1.5 km northwest of the La Flor de La Guajira site (Rollins, 1965).

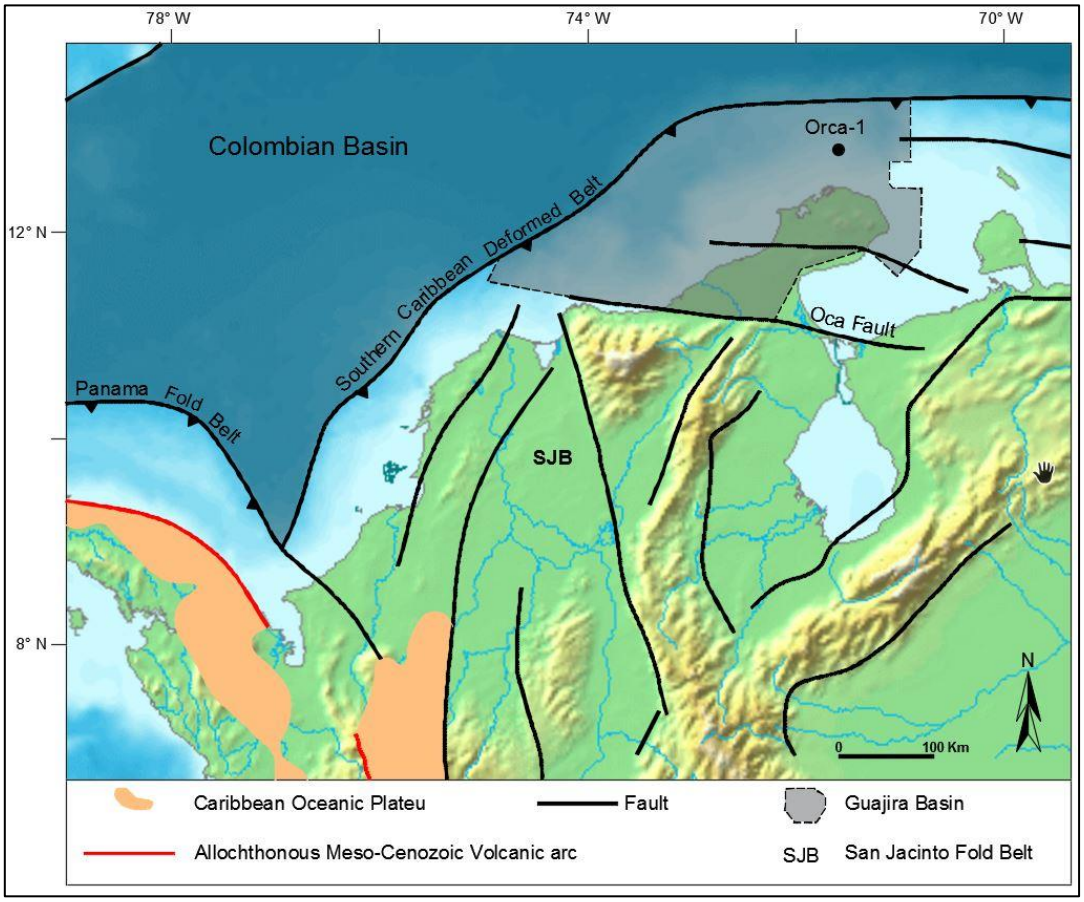

Figure 2. South America and Caribbean region tectonic framework (modified from Cardona et al, 2006).

Siamana Formation: This unit was defined by Renz (1960) as a two-member unit. The lower member comprises limestone conglomerate with clasts of chert, quarzite and metamorphic rocks. The upper member is a limestone with locally reefal developments. Fossils require this unit to have an Oligocene age. Its relationship with the overlying Uitpa Formation varies from unconformable to conformable. The 430 m type section is near Siamana village in the eastern part of Upper Guajira basin.

Uitpa Formation: This unit was defined by Renz (1960) as a lower section comprising abundant calcareous fossiliferous sandstone and locally biostromal limestone, the upper section corresponds to a marly and clayey shale with glauconite, and sandy marl. An upper Oligocene to lower Miocene age was assigned to this unit based on foraminiferal zonations. The type section is located eastward of Siamana village with a thickness that varies from 150 to 200 m. The formation is in conformable contact with the overlying Jimol Formation.

Jimol Formation: This unit was defined by Renz (1960) as a limestone interbedded with marl and shale, locally sandy with quartz, chert and feldspar. The presence of mollusks defined the age as middle Miocene. The 940 m type section is in the central part of the Cosinetas embayment. The formation is in conformable contact with the overlying Castilletes Formation.

Castilletes Formation: This unit was defined by Renz (1960) as a calcareous unit overlain by a mostly clayey section. A Middle to Late Miocene age has been assigned based on biostratigraphic data and stratigraphic position. The type section is in Tucacas Bay with a thickness of 900 m. The formation is in unconformable contact with the overlying Gallinas Formation.

Gallinas Formation: This unit was defined by the Colombian Institute of Geology and Mining (Ingeominas; Ramirez, 2007) in regional geological maps to describe poorly to non-consolidated Pliocene to Pleistocene deposits with fluvial, alluvial, and eolian origins without cartographic differentiation.

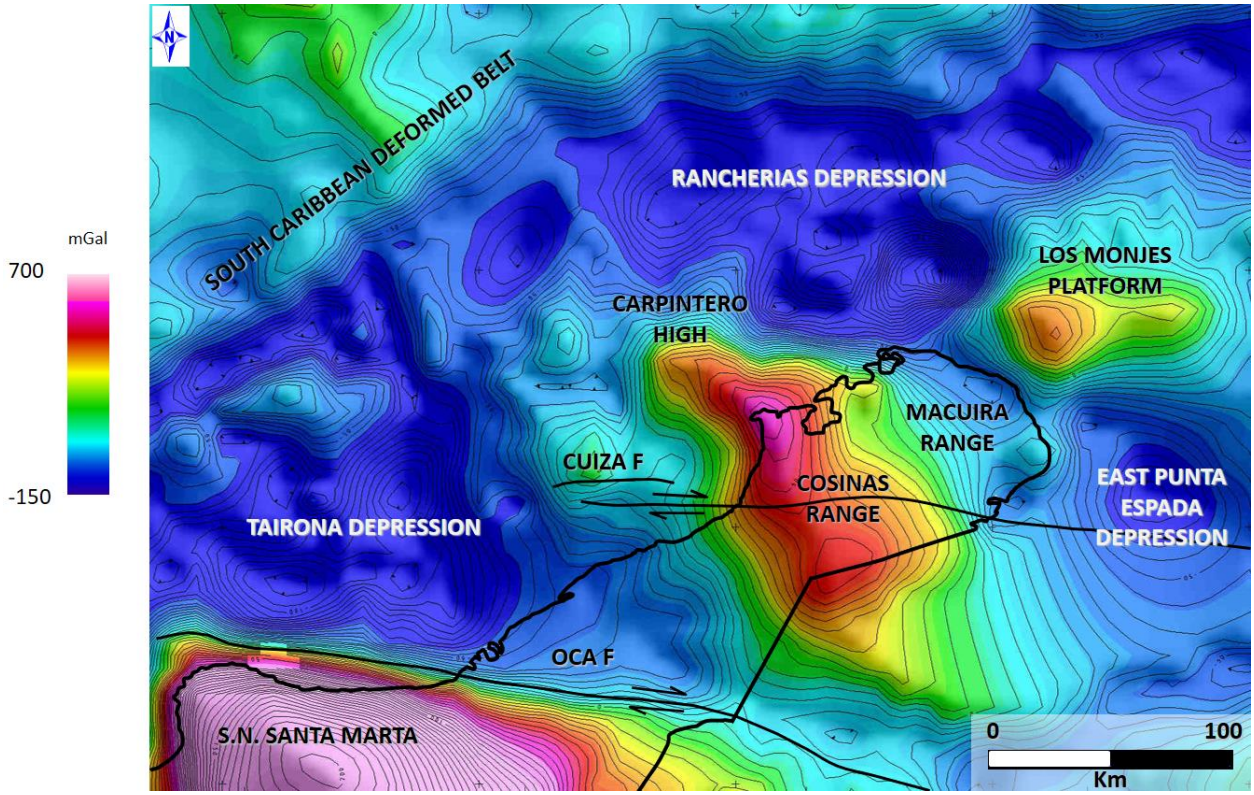

Figure 3. Guajira Basin free-air gravity isostatic anomaly map. Modified from Ceron (2008).

A regional cross section shows the geometry of the basin and the geological relationship between Lower (south) and Upper Guajira (north) subbasins, separated by the dextral strike slip Cuiza fault (Figure 5). The Oligocene horizon identified in onshore Guajira basin, as well as the Lower Magdalena Valley basins, helps to define the main differences in tectonic setting of the stratigraphic record in deepwater Guajira. Pre-Oligocene sequences exhibit deposition in an extensional environment (Ramirez, 2007). The post-Oligocene sequences are deformed by normal faults due to the gravitational collapse that occurred during the collision between the Caribbean and South American plates in Neogene time (Mantilla et al., 2013; Figure 6).

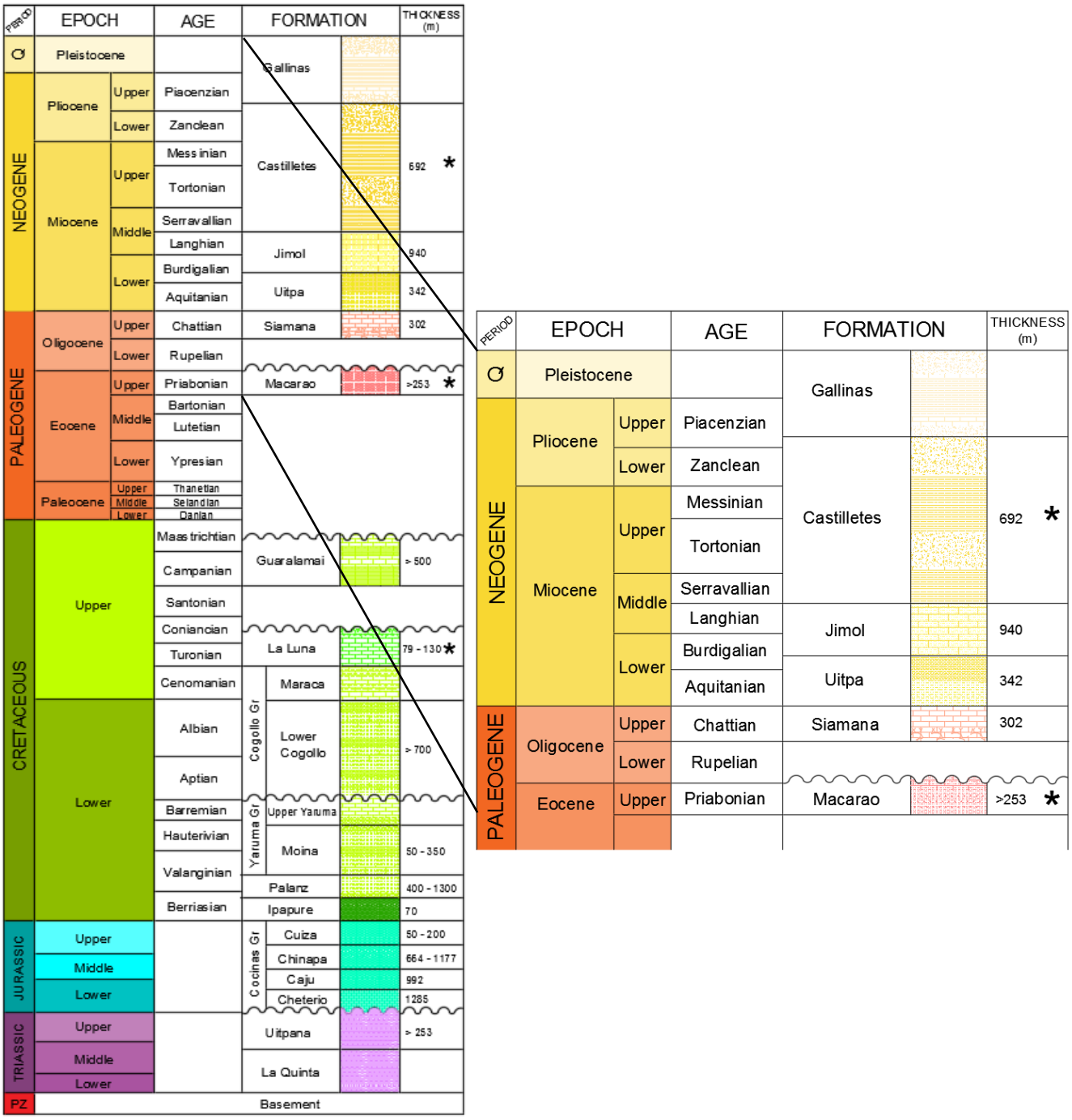

Figure 4. Generalized stratigraphic column for the Guajira Basin. Regional source rocks are indicated by an asterisk (*). Modified from Ramirez (2007).

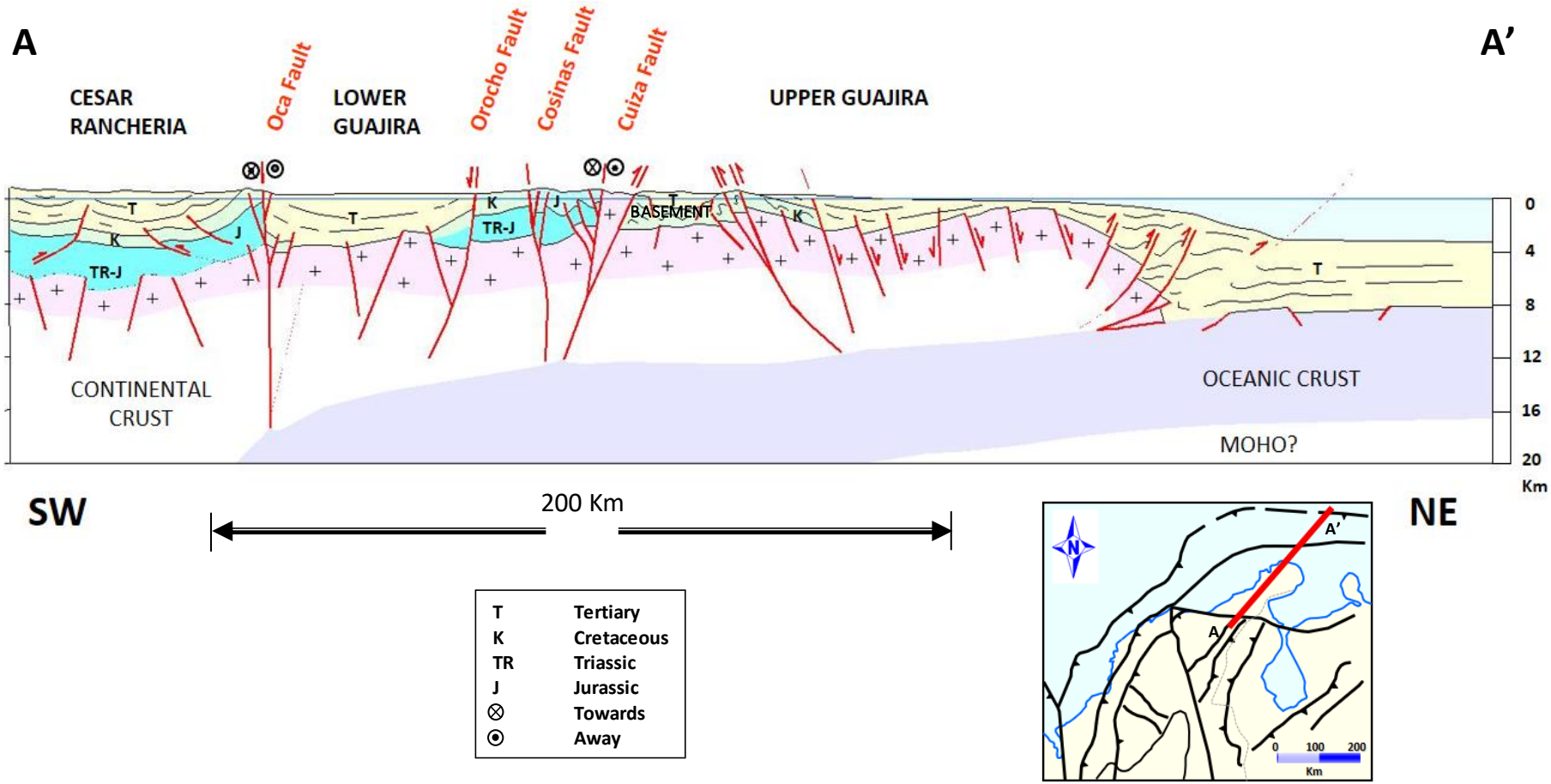

Figure 5. Guajira Basin SW – NE regional cross section. Modified from Ramirez (2007).

Seismic facies characterization assessment, supported by attribute analyses, were used to define the tectono-sequence division made by Mantilla et al. (2013) and delineate the following record of the plate interaction in offshore Guajira (Figure 6):

1. Late Jurassic to Early Cretaceous rift phase during proto-Caribbean opening.
2. Local passive margin deposition during Late Cretaceous time.
3. Late Cretaceous to Paleocene subduction with oceanic terrane accretion.
4. Guajiro and Guarao orogeny during Late Eocene to Early Oligocene time.
5. Eustatic changes caused a Late Oligocene to Early Miocene paraconformity.
6. Deformational event in Late Miocene to Pliocene time related to Caribbean plate subduction under the South American plate as recorded by an angular unconformity.

Paleo-highs formed during Late Eocene to Early Oligocene time and correlation with onshore outcrops support the existence of an Eocene to Oligocene carbonate play related to reservoirs in the Macarao and Siamana Formations (Rubio et al., 2012). Combined traps related to the proposed build-up were mapped, and petroleum system modeling provided enough elements to define drillable prospects in the upper Guajira basin. The best prospect of the ranked portfolio related to the Eocene to Oligocene carbonate play was drilled by the Orca-1 well in 2014 (Petrobras et al., 2012). The reservoir, predicted to be carbonate rocks, was instead a highly laminated sandstone-shale unit (Figure 7) corresponding to intra-slope turbidites in the Siamana Formation.

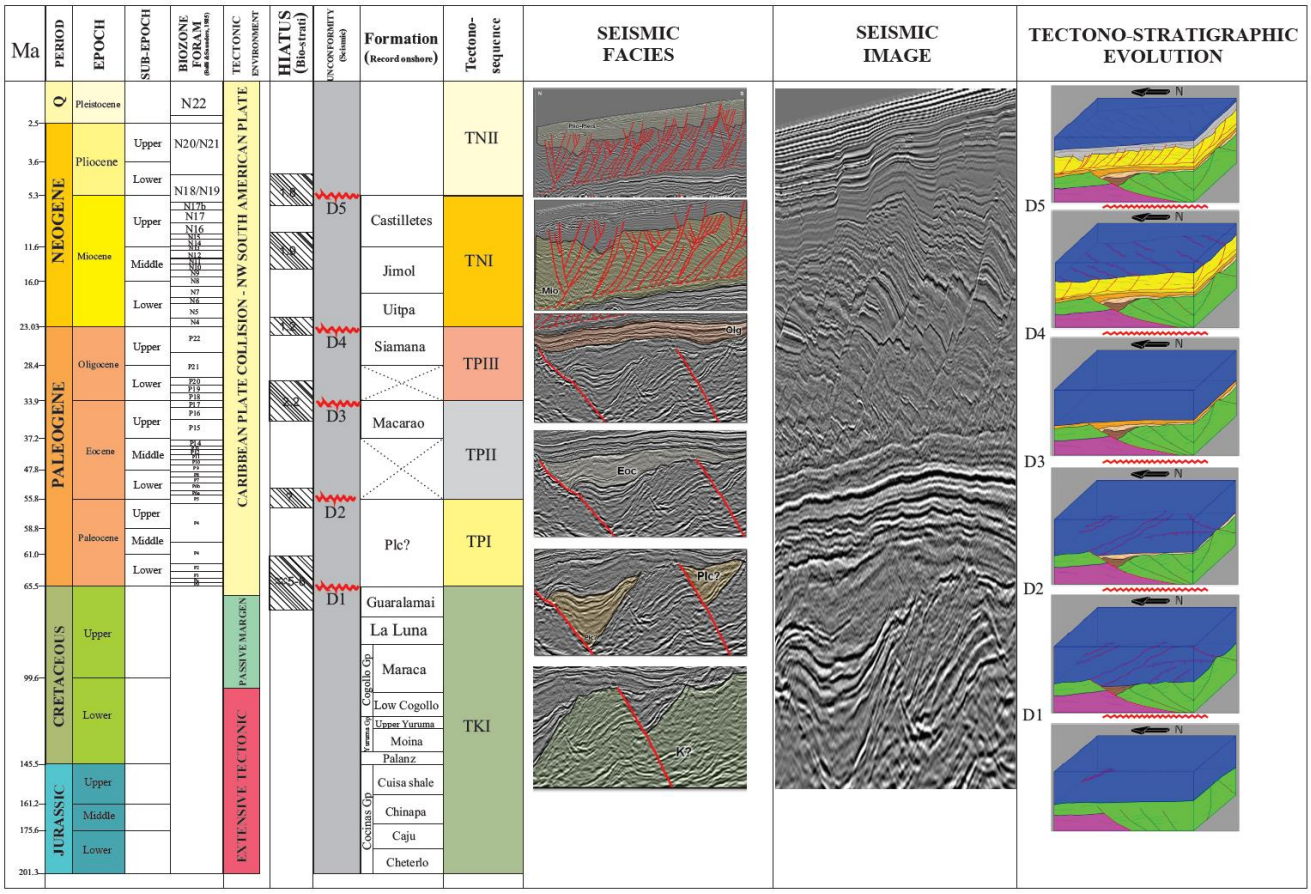

Figure 6. Tectono-sequence division in deepwater Guajira Basin. Modified from Mantilla et al. (2013).

The goal of this study is to create a workflow that is a convenient tool to decrease interpretation uncertainties. This will provide a routine to reduce the time taken for reservoir modeling and development plans for siliciclastic reservoirs. To achieve this goal, the seismic data were reinterpreted to constrain models and the extension of well data. The reservoir characterization used petrophysical properties to calibrate the well data with its seismic expression through seismic attribute analysis and inversion. Seismic attributes, such as

coherence and sweetness, that can differentiate slope deposits in the Guajira Basin, were determined. Reservoir geometry and distribution were defined and mapped to extend the reservoir acoustic impedance beyond the well and into the seismic cube provided for this study. This method could be considered as a best practice in the exploration process, providing a base case to compare seismic amplitudes with well log acoustic impedance. The method can be performed in any kind of reservoir providing fast results towards the understanding of the acoustic impedance changes inside the reservoirs drilled for the first time in frontier basins like Guajira Offshore.

2. METHODS

2.1. Available Data

The data used in this study were provided by Ecopetrol S.A. (Empresa Colombiana de Petroleos). The data are a 1,500 km^2 3-D seismic reflection survey acquired and processed between 2011 and 2012. Table 1 summarizes the acquisition parameters and the processing sequence used for the Jarara 3-D seismic survey. The attribute assessment in this study was carried out using the pre-stack time migration (PSTM) version of the data.

The Orca-1 well, with a total depth of 4,243 m, was drilled between July and September of 2014. It reached its objective at 3,583 m (MD). The drill stem test (DST) performed in the interval 3,583 – 3,617 m (MD) confirmed the hydrocarbon potential in Guajira Basin with gas production of 32 million standard cubic feet of gas per day (MMSCFGD).

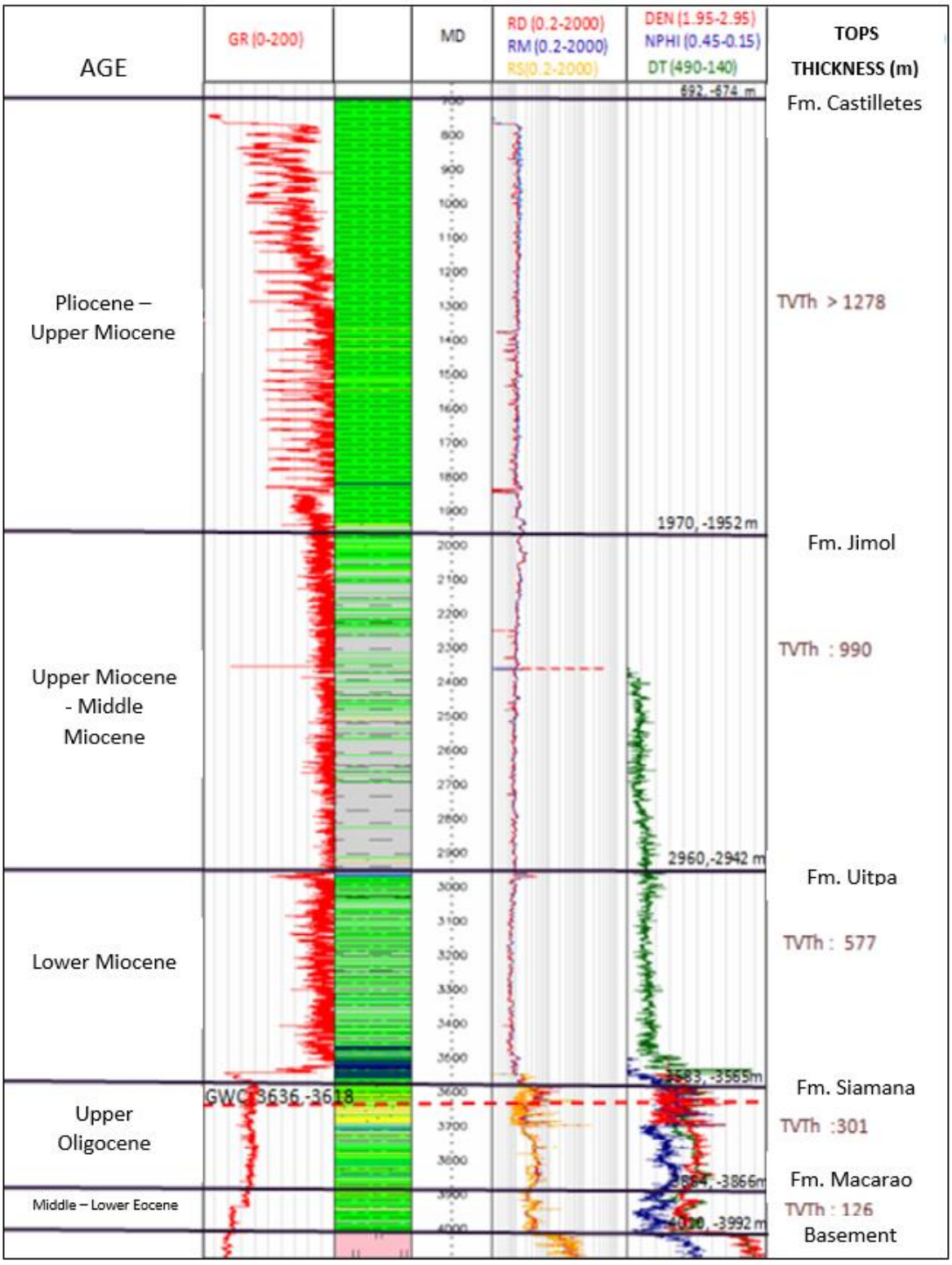

Figure 7. Generalized stratigraphic column for the Orca-1 well. Depths in MD – TVDss. Modified from Petrobras (2015).

Wireline logs (Tables 2 and 3) were used to assess the petrophysical properties of the gas reservoir, such as P- and S-impedance and V_p/V_s ratio, using the Geoview suite of the HampsonRusell® package. Figure 8 shows the location of the Jarara 3-D seismic volume and the Orca-1 well (inline 3,714 – crossline 2,776) to the north of the Guajira peninsula. Additional information such as the well technical summary, geological reviews, regional studies, and internal reports were also provided (Ecopetrol Personal Communication, 2015).

2.2. Approach

Petrel® suite was used to create an interpretation project with the Jarara 3-D seismic reflection survey. Figure 8 shows the seismic inline (1,958 – 5,072) and crossline (172 – 4,276) distribution across the Jarara 3-D survey area, as well as the location of the live traces inside the seismic volume.

The seismic interpretation of the Oligocene horizon was performed in a regular grid (100 inline/crossline spacing) using the seeded 2-D autotracking tool, with 75% seed confidence and a symmetrical constraint over a window width of 5.25 samples per trace. The base of the reservoir was interpreted in a denser grid (10 inline/crossline spacing) using manual interpretation over the acoustic impedance volume generated in Petrel®. The interpreted picks were used to calculate a surface using convergent interpolation and a 12.5 m grid cell size

(inline/crossline spacing). The corresponding structural maps in two-way travel time (TWT) are presented in the results section.

Table 1. Acquisition parameters and general processing sequence – Jarara 3-D survey.

Company	**CGGVeritas**
Vessel Name	Veritas Viking
Full fold area (non-full fold)	1,500 km^2 (1,833 km^2)
Nominal Bin Size	6.25 m x 25 m
Nominal Bin fold	81
Water depths	300 m to 1,500 m
Source parameters	
Source Type	Bolt Long Life Airguns (1500LL and 1900LLX)
Air Pressure	2,000psi+/-100psi
Volume	4,450/in^3
Number of Sources	2
Source separation	50 m
Sub-array separation	8.0 m
Shot Interval	50 m (25 m flip flop)
Source Depth	10 m
Streamer parameters	
Streamer type	Sercel Sentinel Solid
Number of streamers	10
Streamer Depth	10 m
Channels	10 x 648
Streamer separation	100 m
Record Length	9,000 ms
Sample Rate	2 ms
High Cut Filter	200 Hz- 370 dB/Oct
Low Cut Filter	2 Hz - 6 dB/Oct
Group interval	12.5 m
Processing sequence	

Reformatting of seismic from SEGY to CGGV format		
T squared gain recovery		
Low cut 3Hz		
Resampling at 4 ms		
Designature (zero phasing and debubbling)		
Swell noise attenuation		
Linear Noise attenuation		
FK antialias filtering		
Trace drop (dropping one receiver over two)		
3D SRME		
Radon demultiple		
Phase only deabsorption, Q=98		
Source and cable amplitude corrections		
3D de-aliased Fourier interpolation and regularization to a 12.5x12.5m grid		
De-spiking		
Remove T squared gain recovery		
Spherical Divergence Compensation		
PSTM		
Residual Move Out		
Radon demultiple		
Stack and angle stacks		
Spectral whitening		
Dip consistent filtering		
Equalization 2,000 ms window		
PSTM filtered and equalized - gun and cable statics		
Final geometry	**Inlines**	1,958 – 5,073
	Crosslines	172 – 4,276
	Bin size	12.5

Table 2. Orca-1 well wireline logs used in this study.

CURVE	DEPTH INTERVAL (MD)	RUN	DESCRIPTION
GR	1,859 – 2,387 m	3	Gamma Ray (gAPI)
CAL	1,859 – 2,387 m	3	Caliper (in)
RES	2,364- 2,961 m	4	Resistivity (ohm.m)
GR	2,364 – 3,553 m	5	Gamma Ray (gAPI)
CAL	2,364 – 3,553 m	5	Caliper (in)
GR	3,548 – 4,238 m	8	Calibrated Gamma Ray (gAPI)
CAL	3,548 – 4,238 m	8	Caliper (in)
SP	3,548 – 4,238 m	8	Spontaneous Potential (mV)
TNPH	3,548 – 4,238 m	8	Thermal Neutron Porosity (m^3/m^3)
RHOZ	3,548 – 4,238 m	8	Standard Resolution Formation Density (gr/cm^3)
RT	3,548 – 4,238 m	8	True Resistivity (ohm.m)
RXO	3,548 – 4,238 m	8	Flushed Zone Resistivity (ohm.m)
DTCO	3,548 – 4,238 m	8	Delta-T Compressional (us/ft)
DTSM	3,548 – 4,238 m	8	Delta-T Shear (us/ft)
CHECKSHOT	693 – 4,237 m	-	Borehole Seismic data
FMI - UBI	3,568 – 4,010 m	-	Formation Microimager - Ultrasonic Imager
MDT	3,580 – 3,690 m	-	Modular Formation Dynamics Tester
DST	3,583 – 3,617 m	-	Drill Stem Test

Table 3. Orca-1 well checkshot data used in this study (Petrobras, 2015).

Well coordinates

East (m)	North (m)	RT Elev. [m] @msl		GL Elev. [m] @msl
1269402.160	1906718.604	18.00		-675.00

Source coordinates

East (m)	North (m)	Elevation [m] @msl
1269402.106	1906782.604	-5.00

Datum [m amsl] 0.0

Replacement Velocity (constant) [m/s]	rv=	1500.00
Seismic Reference Datum from RT (constant) [m]	d=	18.0
Vertical Distance from RT to Source (constant) [m]	sz=	23.0
Eastwards Horizontal Offset from Wellhead to Source (constant) [m]	wse=	-0.1
Northwards Horizontal Offset from Well to Source (constant) [m]	wsn=	64.0

Petrobras Colombia
EXPLORATION DEPARTMENT

Orca-1
VELOCITY REPORT

Date of run: **Oct. 04/14** Date of report delivery: **Oct. 06/14**

GENERAL GEOMETRY

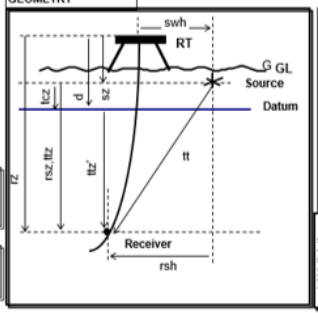

Well to Source offset: [m] 64.0

Well to Source azimuth: [deg] 360.0

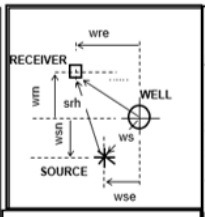

SOURCE: Airgun
TOOL: VSI
ACQ. SYSTEM: MAXIS 500
CONTRACTOR: Schlumberger
WITNESS:

DISTRIBUTION LIST:
1.
2.
3.
4.
5.

DEFINITIONS TABLE

RT: Rotary Table
GL: Ground Level
rv: replacement velocity [ft/s]
d : Vertical distance from RT to Datum
sz : Vertical Distance from RT to Source
rz : Vertical Distance from RT to Receiv.

wsh : Horizontal Distance from Source to Wellhead
wse : East offset from Source to Wellhead
wsn : North offset from Source to Wellhead
wre : East offset from Receiver to Wellhead
wrn : North offset from Receiver to Wellhead
srh : Horizontal Distance from Source to Receiver

tt :Travel Time from Source to Receiver
ttz :Vertical Travel Time from Source to Receiver
tcz :Vertical Correction Time from Source to Datum
ttz' :Vertical Travel Time from Datum to Source
av :Average Velocity from Datum
iv : Interval Velocity

SIGN CONVENTION:
Eastwards, Northwards and Downwards distances are positive.
Downwards time is positive.

NOTE:
Unless it be specified, all distances are in feet from RT.

Vertical Correction Time from Source to Datum [ms]	tcz=	-3.333

Datum [m amsl]=> 0.0

Vertical well

Tops (Comments)	Receiver Measured Depth [m]	Receiver Vertical Depth (Deviation Survey) [m]	Receiver Vertical Depth (Deviation Survey) from Datum [m]	East Offset from Well to Receiver (Deviation Survey) [m]	North Offset from Well to Receiver (Deviation Survey) [m]	Horizontal Offset from Source to Receiver (computed) [m]	Vertical Offset from Source to Receiver (computed) [m]	* Bad pick (?)	Travel Time from Source to Receiver (measured) [ms]	Vertical Travel Time from Source to Receiver (computed) [ms]	Vertical Travel Time from Datum (computed) [ms]	Average Velocity from Datum (computed) [m/s]	Interval Velocity (computed) [m/s]
	r	rz	rz'	wre	wrn	srh	srz		tt	ttz	ttz'	av	iv
	692.99	692.99	674.99	0.00	0.00	64.0	670.0		445.00	443.0	446.3	1,512	
													1,818
	748.77	748.77	730.77	0.00	0.00	64.0	725.8		475.50	473.7	477.0	1,532	
													1,821
	1349.93	1349.93	1331.93	0.00	0.00	64.0	1326.9		804.65	803.7	807.0	1,650	
													1,893
	1999.96	1999.96	1981.96	0.00	0.00	64.0	1977.0		1147.69	1,147.1	1,150.4	1,723	
													2,012
	2214.98	2214.98	2196.98	0.00	0.00	64.0	2192.0		1254.50	1,254.0	1,257.3	1,747	
													2,147
	2375.02	2375.02	2357.02	0.00	0.00	64.0	2352.0		1329.00	1,328.5	1,331.8	1,770	
													2,181
	2959.99	2959.99	2941.99	0.00	0.00	64.0	2937.0		1597.05	1,596.7	1,600.0	1,839	
													2,308
	3187.98	3187.98	3169.98	0.00	0.00	64.0	3165.0		1695.81	1,695.5	1,698.8	1,866	
													2,366
	3203.10	3203.10	3185.10	0.00	0.00	64.0	3180.1		1702.20	1,701.9	1,705.2	1,868	
													2,397
	3218.68	3218.68	3200.68	0.00	0.00	64.0	3195.7		1708.70	1,708.4	1,711.7	1,870	
													2,418
	3233.80	3233.80	3215.80	0.00	0.00	64.0	3210.8		1714.95	1,714.6	1,717.9	1,872	
													2,279
	3248.92	3248.92	3230.92	0.00	0.00	64.0	3225.9		1721.58	1,721.2	1,724.6	1,873	
													2,221

	3264.04	3264.04	3246.04	0.00	0.00	64.0	3241.0	1728.39	1,728.0	1,731.4	1,875	
2,281												
	3279.75	3279.75	3261.75	0.00	0.00	64.0	3256.7	1735.27	1,734.9	1,738.3	1,876	
2,246												
	3294.87	3294.87	3276.87	0.00	0.00	64.0	3271.9	1742.00	1,741.7	1,745.0	1,878	
2,267												
	3309.99	3309.99	3291.99	0.00	0.00	64.0	3287.0	1748.67	1,748.3	1,751.7	1,879	
2,251												
	3325.11	3325.11	3307.11	0.00	0.00	64.0	3302.1	1755.39	1,755.1	1,758.4	1,881	
2,181												
	3340.63	3340.63	3322.63	0.00	0.00	64.0	3317.6	1762.50	1,762.2	1,765.5	1,882	
2,200												
	3355.75	3355.75	3337.75	0.00	0.00	64.0	3332.8	1769.37	1,769.0	1,772.4	1,883	
2,292												
	3370.87	3370.87	3352.87	0.00	0.00	64.0	3347.9	1775.97	1,775.6	1,779.0	1,885	
2,267												
	3385.99	3385.99	3367.99	0.00	0.00	64.0	3363.0	1782.64	1,782.3	1,785.6	1,886	
2,261												
	3401.64	3401.64	3383.64	0.00	0.00	64.0	3378.6	1789.56	1,789.2	1,792.6	1,888	
2,287												
	3416.76	3416.76	3398.76	0.00	0.00	64.0	3393.8	1796.17	1,795.8	1,799.2	1,889	
2,284												
	3431.88	3431.88	3413.88	0.00	0.00	64.0	3408.9	1802.79	1,802.5	1,805.8	1,891	
2,238												
	3447.00	3447.00	3429.00	0.00	0.00	64.0	3424.0	1809.54	1,809.2	1,812.6	1,892	
2,139												
	3462.53	3462.53	3444.53	0.00	0.00	64.0	3439.5	1816.80	1,816.5	1,819.8	1,893	
2,099												
	3477.65	3477.65	3459.65	0.00	0.00	64.0	3454.7	1824.00	1,823.7	1,827.0	1,894	
2,247												
	3492.77	3492.77	3474.77	0.00	0.00	64.0	3469.8	1830.73	1,830.4	1,833.7	1,895	
2,299												
	3507.89	3507.89	3489.89	0.00	0.00	64.0	3484.9	1837.30	1,837.0	1,840.3	1,896	
2,583												
	3523.49	3523.49	3505.49	0.00	0.00	64.0	3500.5	1843.34	1,843.0	1,846.4	1,899	
2,419												
	3538.61	3538.61	3520.61	0.00	0.00	64.0	3515.6	1849.59	1,849.3	1,852.6	1,900	
2,504												
	3553.73	3553.73	3535.73	0.00	0.00	64.0	3530.7	1855.63	1,855.3	1,858.7	1,902	
2,618												
	3568.85	3568.85	3550.85	0.00	0.00	64.0	3545.9	1861.40	1,861.1	1,864.4	1,905	
2,642												
	3584.49	3584.49	3566.49	0.00	0.00	64.0	3561.5	1867.32	1,867.0	1,870.3	1,907	
2,444												
	3599.61	3599.61	3581.61	0.00	0.00	64.0	3576.6	1873.50	1,873.2	1,876.5	1,909	
2,466												
	3614.73	3614.73	3596.73	0.00	0.00	64.0	3591.7	1879.63	1,879.3	1,882.7	1,910	
2,816												
	3629.85	3629.85	3611.85	0.00	0.00	64.0	3606.8	1885.00	1,884.7	1,888.0	1,913	
3,059												
	3645.45	3645.45	3627.45	0.00	0.00	64.0	3622.5	1890.10	1,889.8	1,893.1	1,916	
2,652												
	3660.57	3660.57	3642.57	0.00	0.00	64.0	3637.6	1895.80	1,895.5	1,898.8	1,918	
2,438												
	3675.69	3675.69	3657.69	0.00	0.00	64.0	3652.7	1902.00	1,901.7	1,905.0	1,920	
2,571												
	3690.81	3690.81	3672.81	0.00	0.00	64.0	3667.8	1907.88	1,907.6	1,910.9	1,922	
3,530												
	3706.43	3706.43	3688.43	0.00	0.00	64.0	3683.4	1912.30	1,912.0	1,915.3	1,926	
2,652												
	3721.55	3721.55	3703.55	0.00	0.00	64.0	3698.5	1918.00	1,917.7	1,921.0	1,928	
3,023												
	3736.67	3736.67	3718.67	0.00	0.00	64.0	3713.7	1923.00	1,922.7	1,926.0	1,931	
3,357												
	3751.79	3751.79	3733.79	0.00	0.00	64.0	3728.8	1927.50	1,927.2	1,930.6	1,934	
2,817												
	3767.33	3767.33	3749.33	0.00	0.00	64.0	3744.3	1933.02	1,932.7	1,936.1	1,937	
2,936												
	3782.45	3782.45	3764.45	0.00	0.00	64.0	3759.5	1938.17	1,937.9	1,941.2	1,939	
2,988												
	3797.57	3797.57	3779.57	0.00	0.00	64.0	3774.6	1943.23	1,942.9	1,946.3	1,942	
3,034												
	3812.69	3812.69	3794.69	0.00	0.00	64.0	3789.7	1948.21	1,947.9	1,951.3	1,945	
3,021												
	3828.38	3828.38	3810.38	0.00	0.00	64.0	3805.4	1953.40	1,953.1	1,956.5	1,948	
3,042												
	3843.50	3843.50	3825.50	0.00	0.00	64.0	3820.5	1958.37	1,958.1	1,961.4	1,950	
3,236												
	3858.62	3858.62	3840.62	0.00	0.00	64.0	3835.6	1963.04	1,962.8	1,966.1	1,953	
3,202												
	3873.74	3873.74	3855.74	0.00	0.00	64.0	3850.7	1967.76	1,967.5	1,970.8	1,956	
2,694												
	3889.21	3889.21	3871.21	0.00	0.00	64.0	3866.2	1973.50	1,973.2	1,976.6	1,959	
2,519												
	3904.33	3904.33	3886.33	0.00	0.00	64.0	3881.3	1979.50	1,979.2	1,982.6	1,960	
2,353												
	3919.45	3919.45	3901.45	0.00	0.00	64.0	3896.5	1985.92	1,985.7	1,989.0	1,962	
3,258												
	3934.57	3934.57	3916.57	0.00	0.00	64.0	3911.6	1990.56	1,990.3	1,993.6	1,965	
2,956												
	3969.97	3969.97	3951.97	0.00	0.00	64.0	3947.0	2002.53	2,002.3	2,005.6	1,970	
2,832												
	4006.97	4006.97	3988.97	0.00	0.00	64.0	3984.0	2015.60	2,015.3	2,018.7	1,976	
5,464												
	4099.91	4099.91	4081.91	0.00	0.00	64.0	4076.9	2032.60	2,032.3	2,035.7	2,005	
5,864												
	4175.01	4175.01	4157.01	0.00	0.00	64.0	4152.0	2045.40	2,045.2	2,048.5	2,029	
5,533												
	4237.01	4237.01	4219.01	0.00	0.00	64.0	4214.0	2056.60	2,056.4	2,059.7	2,048	

The Geoview suite of the HampsonRusell® package was used to perform a well to seismic tie and post-stack inversion analysis from the PSTM version of the Jarara 3-D seismic reflection survey and Orca-1 well log data. Seismic inversion takes computed impedance values from well data and the seismic trace to generate an integrated trace as a better representation of the geologic features acting as reflectors in the subsurface (Figure 9). The resulting inversion shows the lithologic boundaries causing changes in acoustic impedance.

Geoview® suite offers different methods to model the seismic data considering the correlation between the initial model (from well data) and the synthetic inversion (acoustic impedance values after inversion). Model based and colored post-stack inversion methods were analyzed in this study. Model based inversion creates a P-impedance low frequency model by searching for a good fit with the original data by modifying the initial parameters, such as wavelet, block size, number of iterations and constraint windows. Colored inversion creates an operator that considers both the spectrum from seismic amplitudes and acoustic impedance from well logs. In this sense, colored inversion is consistent with the acoustic impedance trend in the area regarding the data available from the well. In both cases, the final product is an acoustic impedance volume with absolute values in the first case and relative values in the second case. The seismic interpretation was used to constrain the inversion modeling that was extrapolated into the seismic volume.

Seismic attributes were computed using a cropped volume of the original data to obtain better performance and visualization. The new volume was optimized along inline 2,600 – 4,550,

crossline 960 – 3,369 and in the depth range of 3,000 – 6,000 ms. Different attribute volumes were generated using Petrel's algorithms to evaluate the seismic response of the reservoir and its continuity in the study area.

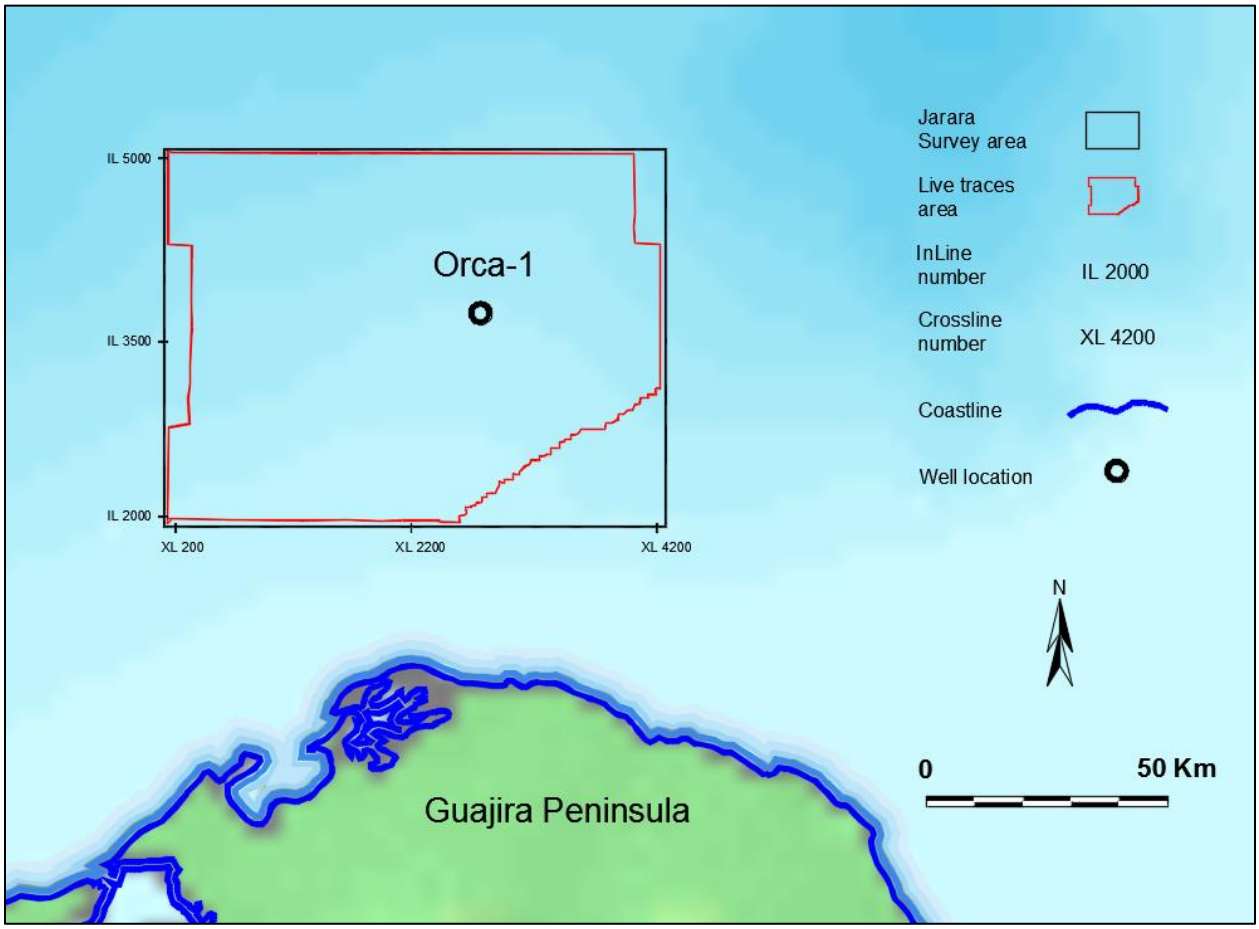

Figure 8. Jarara 3-D seismic survey and the location of the Orca-1 well in the offshore Guajira Basin.

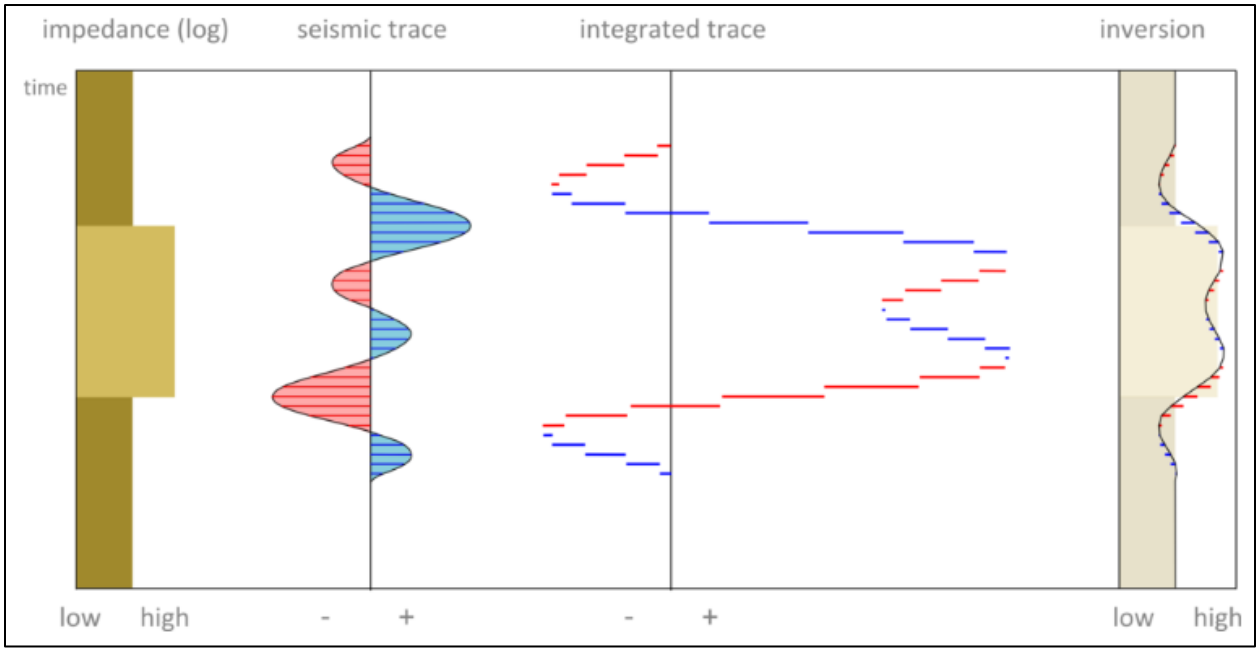

Figure 9. The principle of seismic inversion. The integrated trace represents the geologic features generating reflections in the subsurface (Bianco, 2011).

3. RESULTS

3.1. Well to seismic tie

Wireline well log curves were used to compute the elastic properties of the siliciclastic gas reservoir. Figure 10 shows P- and S-impedance, as well as gamma ray, density and V_p/V_s ratio values characterizing the reservoir.

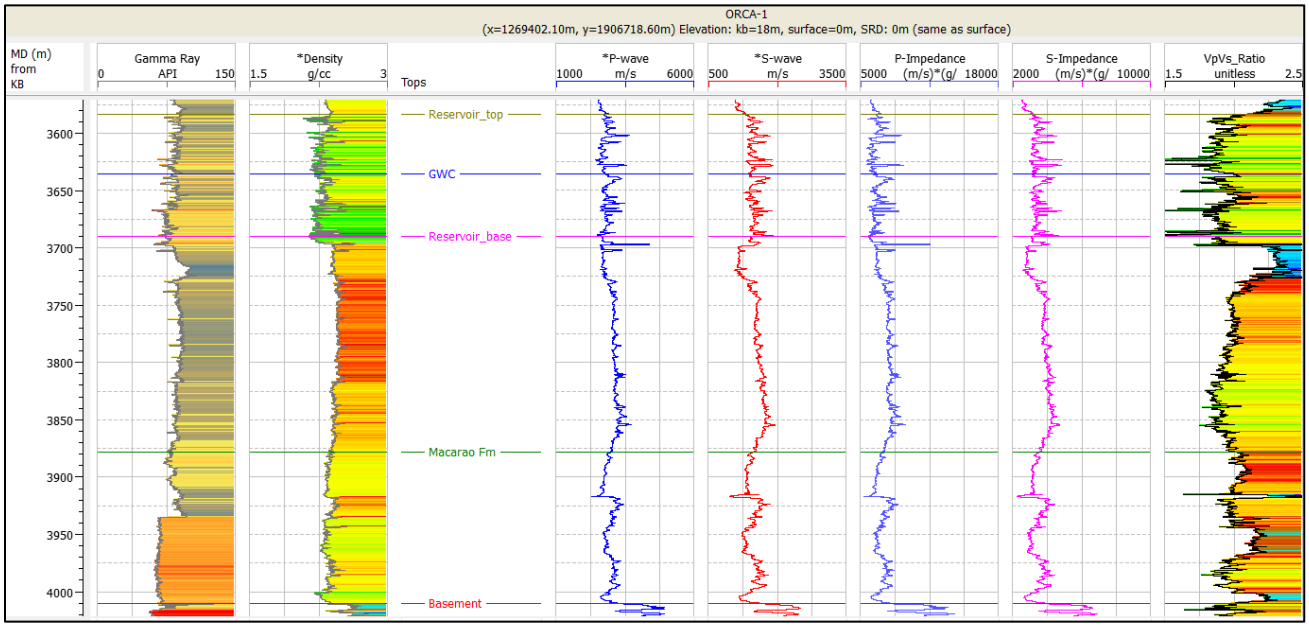

Figure 10. Elastic properties of the Orca-1 well. Tops, indicating the reservoir location, as well as basement, are annotated. GWC = gas water contact.

Given the variations in acoustic impedance due to the thin bedded reservoir, sonic velocities were corrected using checkshot velocities (Table 3) to calculate the synthetic seismogram and well correlation (Figure 11).

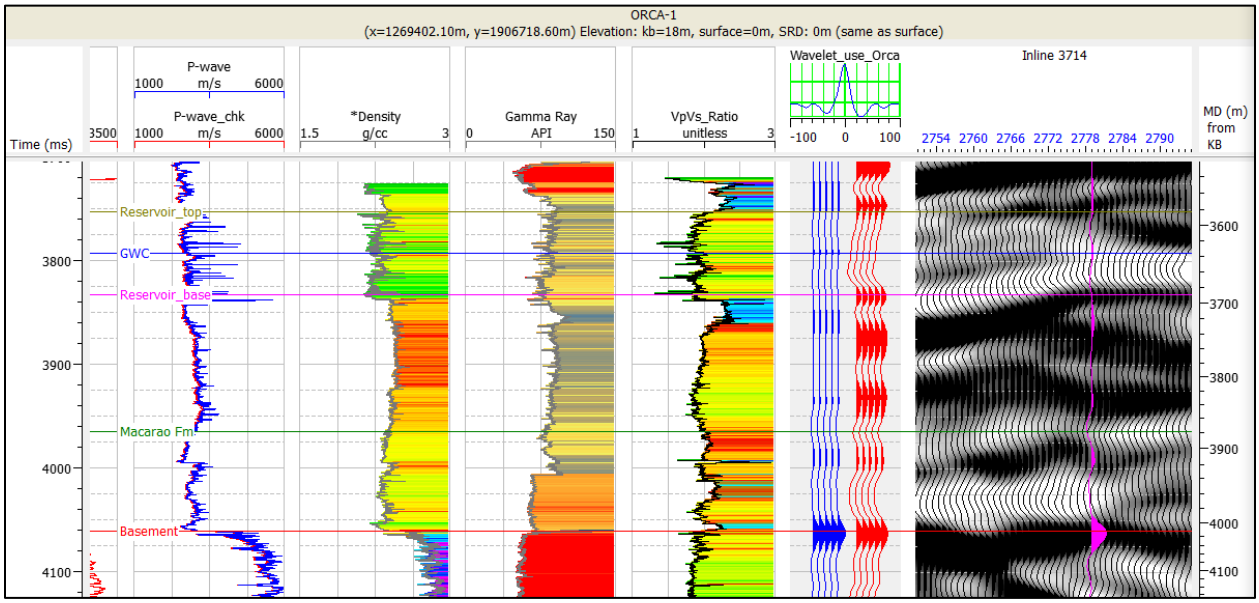

Figure 11. Orca-1 well synthetic seismogram, Guajira offshore.

3.2. Seismic attributes

Considering the low frequency of the seismic data (15 Hz) at the reservoir depth (3,600 – 4,000 ms), the stratigraphic attribute of relative acoustic impedance (RAI) provided a better image of lateral changes in lithology and discontinuities, by showing an apparent acoustic contrast in the seismic section. This is helpful in interpreting the boundaries inside seismic facies

(Chopra and Marfurt, 2007). Figure 12 compares an image obtained using seismic amplitudes (a) to an image comprising relative acoustic impedance (b) for the same seismic section. The well path is projected (dashed line) so that the differences in the reservoir zone (Figure 10) are highlighted. Stratigraphic bodies (red circle) are better defined when using relative acoustic impedance (RAI).

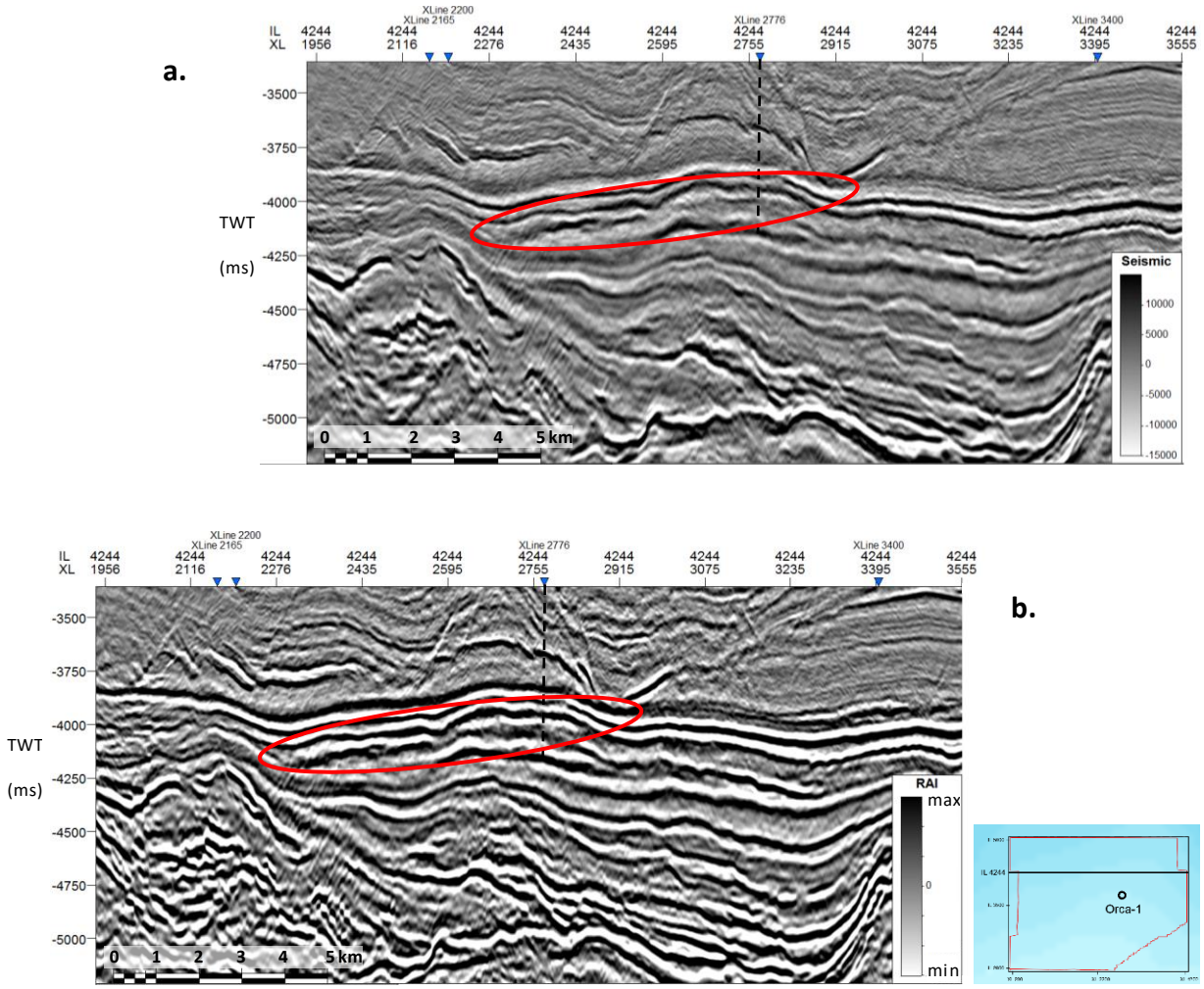

Figure 12. Inline 4,244 without interpretation. Seismic amplitudes (a) are compared to relative acoustic impedance (b). Note the better definition of boundaries and discontinuities inside the same seismic facies in the relative acoustic impedance section (RAI).

The relative acoustic impedance volume (RAI) was used to interpret the base of the reservoir using manual interpretation to avoid the inclusion of non-related bodies. The green shaded polygon in Figure 13 illustrates additional thickness in the reservoir when the interpretation is done using just seismic amplitudes.

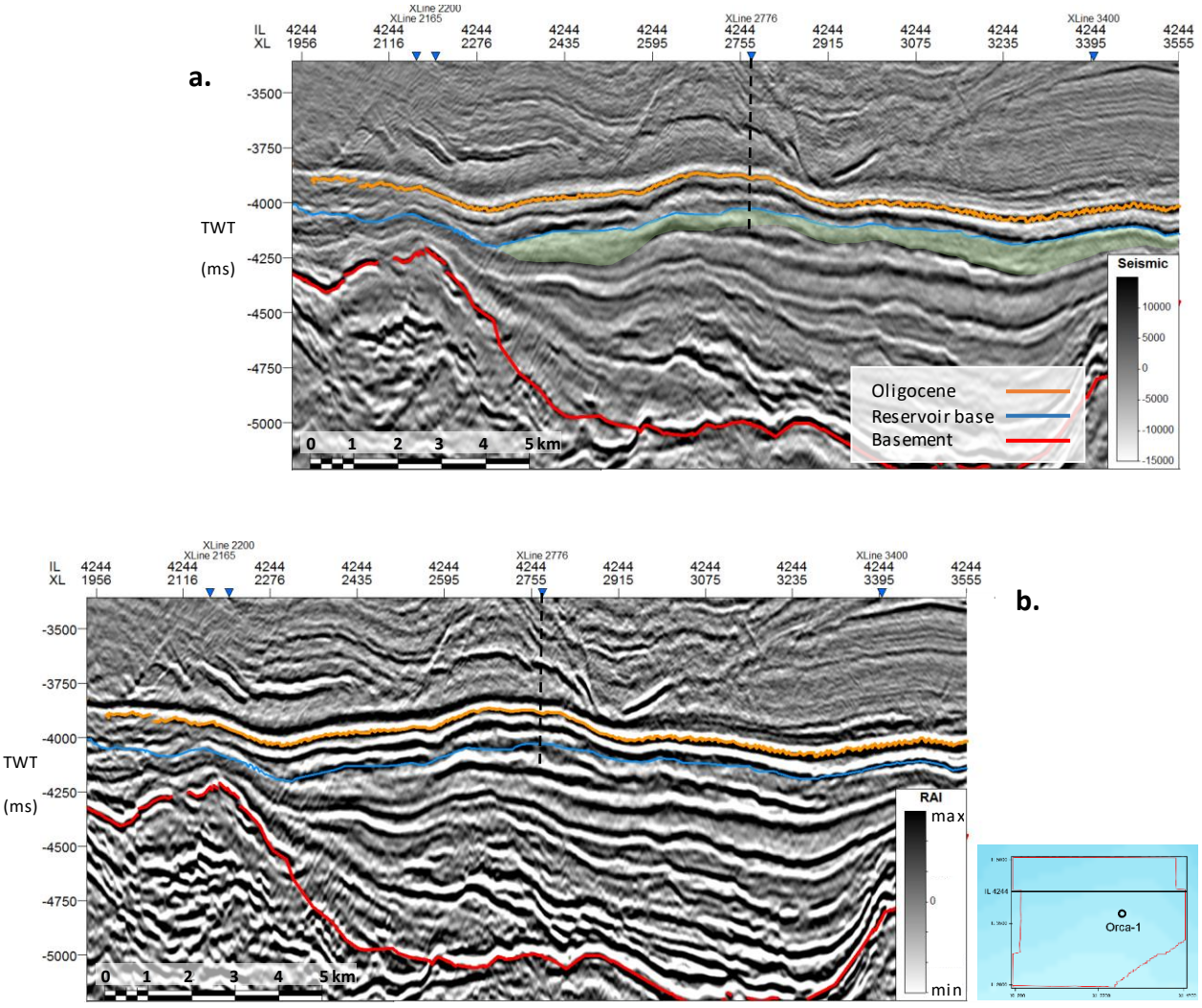

Figure 13. Inline 4,244 with interpretation using seismic amplitudes (a) and the RAI volume (b). Note the extra thickness (green shaded area) that could be erroneously attributed to the reservoir zone if interpretation was made using the seismic amplitude volume.

Coherence, another stratigraphic attribute, is the similarity between seismic traces. High values of coherence are indicative of consistency between a trace and its neighbors based on dip and azimuth analysis. In clastic prone environments, this attribute is frequently used to enhance channel infill and channel system edges, as well as seismic facies geometry and fault/fracture recognition (Chopra and Marfurt, 2007). Figure 14 shows maximum values of coherence (red arrows) related to fine-grained sedimentary rocks drilled by the Orca-1 well, over and under the Oligocene marker; where reflectors are parallel and laterally continuous and high amplitude. Paleo-highs are covered with onlap terminations that are regionally distributed. The reservoir section exhibits high coherence values without prominent edges or internal changes related to major faulting.

Bacon et al. (2007) defined the seismic attribute of envelope as the maximum value of the trace, at a given time, if the phase were rotated (instantaneous phase). This attribute is phase independent and always positive. The envelope attribute is a representation of reflectivity along the seismic section, being comparable with changes in acoustic impedance. The envelope attribute is used to identify boundaries, small changes in thickness and lateral changes in lithology. The attribute of envelope in Figure 15 shows the lateral continuity of the Oligocene and Miocene sequences overlying the Oligocene reservoir. The reservoir has continuity inside the drilled structure with internal changes that allow differentiation of its geometry and lateral extent.

The sweetness attribute is a direct relationship between envelope and instantaneous frequency. It is useful in differentiating sandstone bodies surrounded by shaly sequences (Hart, 2008). Sweetness works in siliciclastic environments as a hydrocarbon indicator. It highlights high envelope/low frequency sand bodies with hydrocarbons (high sweetness, or "sweet spots") from typically fine-grained sequences that act as seal units, with low envelope/high frequency values (low sweetness). In the Jarara 3-D volume, the sweetness attribute has a high correlation with envelope, distinguishing the reservoir inside the drilled structure from the fine-grained sequences defined as seal rock. This permits a regional interpretation of this property away from the borehole (Figure 16).

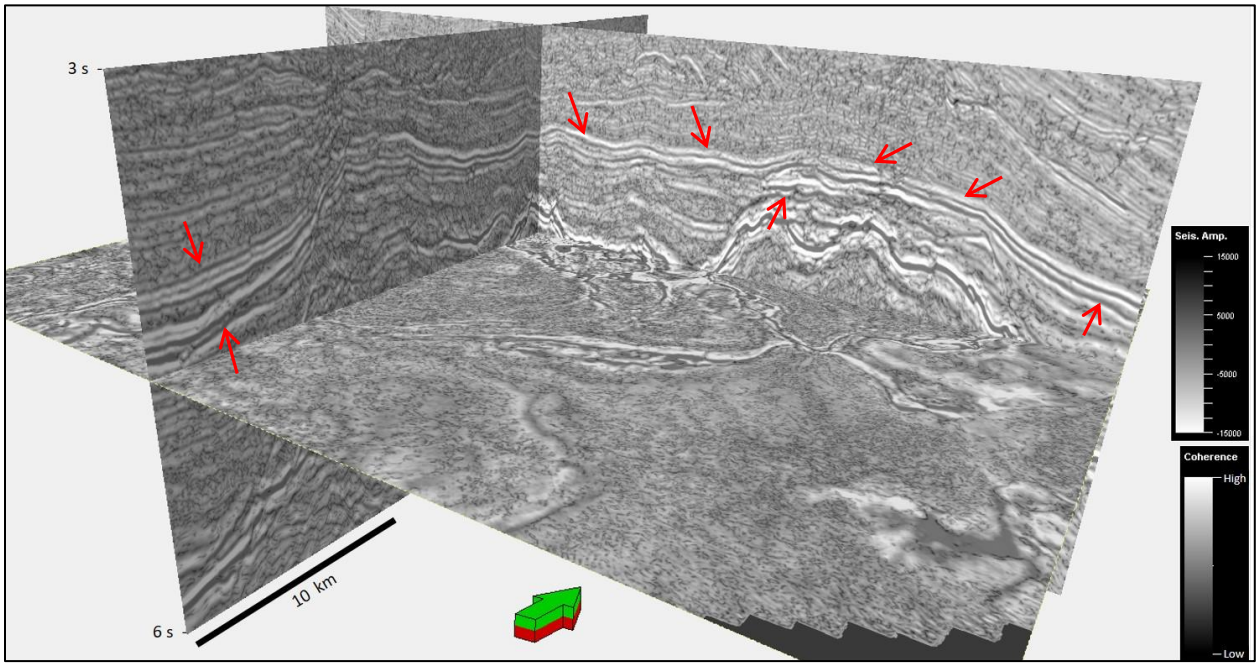

Figure 14. Coherence attribute co-rendered with seismic amplitude for the inline 3,714, crossline 2,000, and 4,500 ms time slice intersection. The arrow points north and green is up.

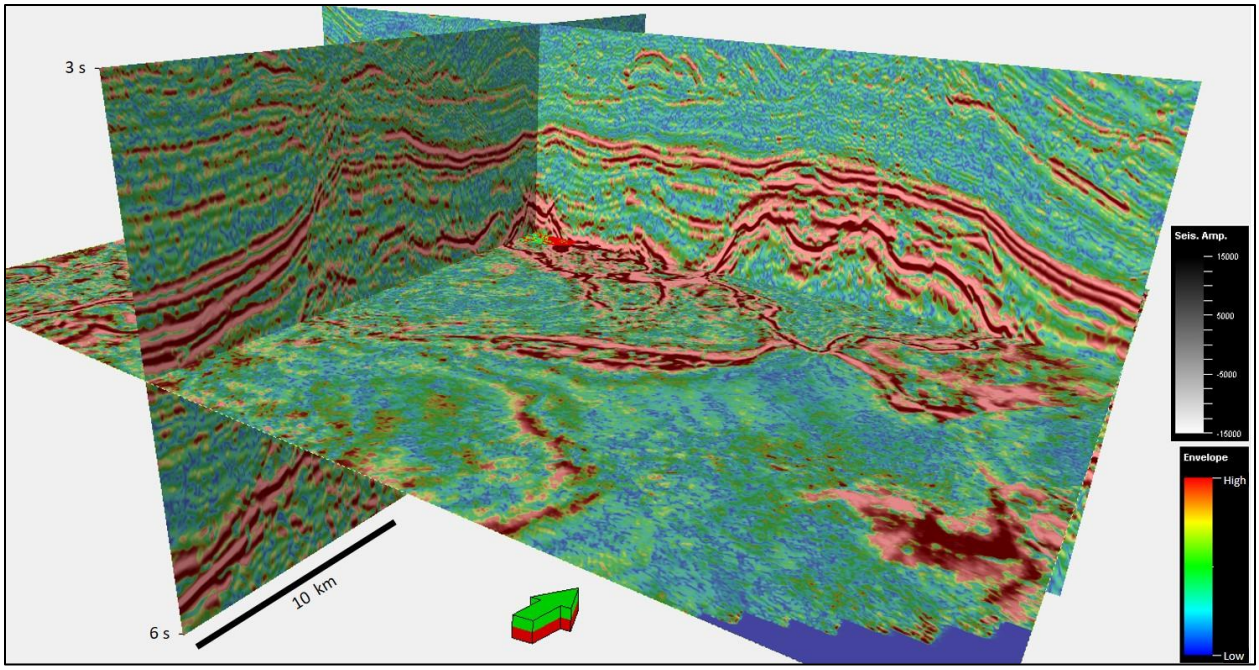

Figure 15. Envelope attribute co-rendered with seismic amplitude for the inline 3,714, crossline 2,000, and 4,500 ms time slice intersection. The arrow points north and green is up.

The seismic frequency content discrimination helps to identify the influence of each frequency value in the seismic volume. In siliciclastic environments, this aids in recognition of thin beds, channelized features, and lateral changes in lithologies to obtain thickness estimates (with low frequencies showing only thicker channels; Chopra and Marfurt, 2007). Using Petrel's IsoFrequency attribute, three cubes with spectral components were calculated. Figure 17 shows IsoFrequency volumes (red - 16 Hz, green - 11 Hz, and blue - 6 Hz with a correlation window of 60 ms each) co-rendered with seismic amplitude (vertically) and coherence (time slice). In the case of the Jarara 3-D volume, very little correlation was found between the frequency content and the lithology analyzed as the reservoir. Some of the areas inside the reservoir are illuminated by red and blue frequencies (16 and 6 Hz), but the map view at the reservoir level (3,732 ms)

does not permit interpretation of geometry or distribution of events related to the deposition of turbidites in the area (Figure 18).

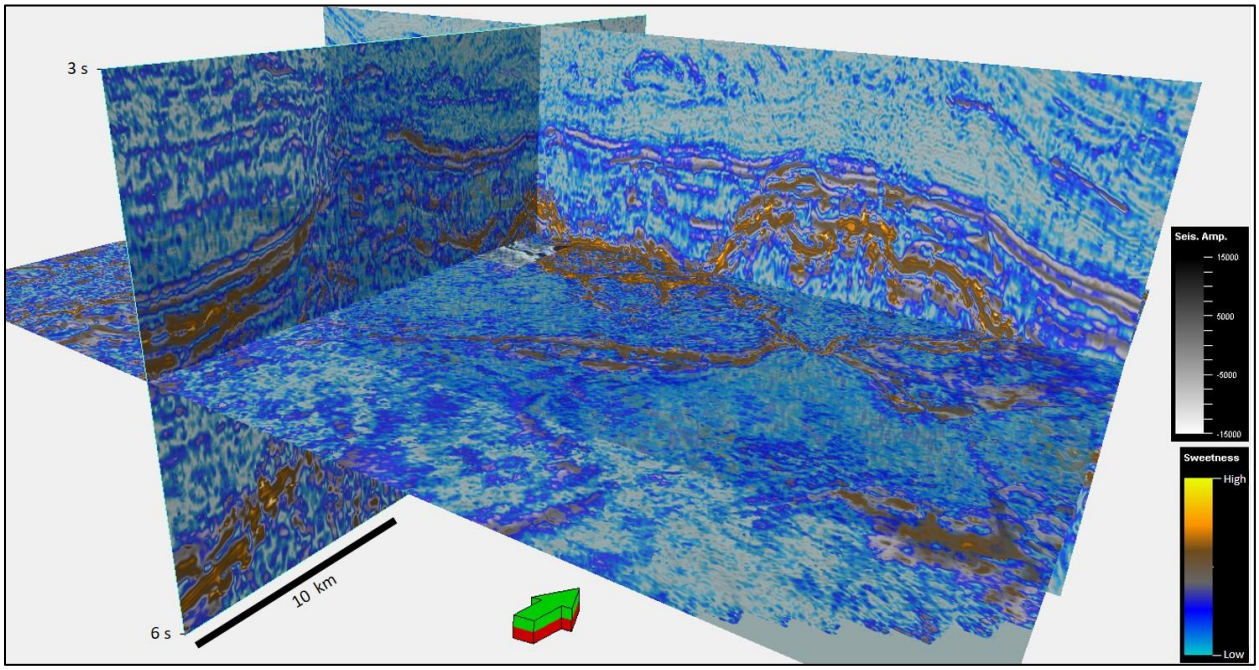

Figure 16. Sweetness attribute co-rendered with seismic amplitude for the inline 3,714, crossline 2,000, and 4,500 ms time slice intersection. The arrow points north and green is up.

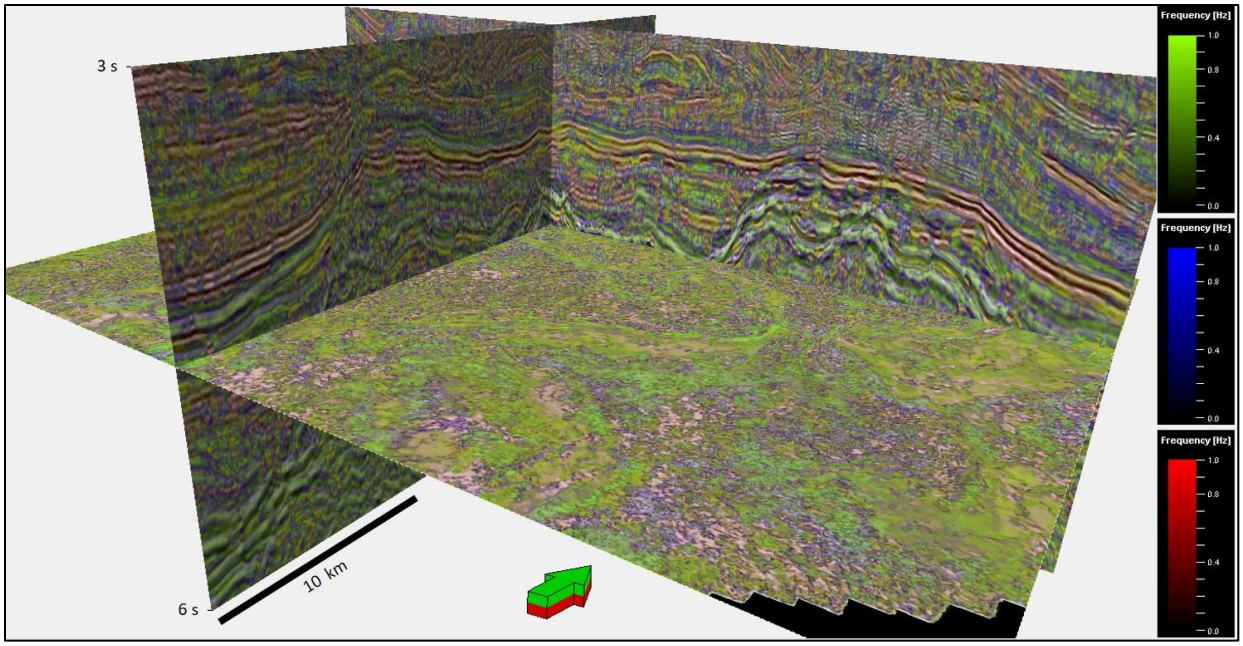

Figure 17. IsoFrequency attribute co-rendered with seismic amplitude (vertical) and coherence (time slice), for the inline 3,714, crossline 2,000, and 4,500 ms time slice intersection. The arrow points north and green is up.

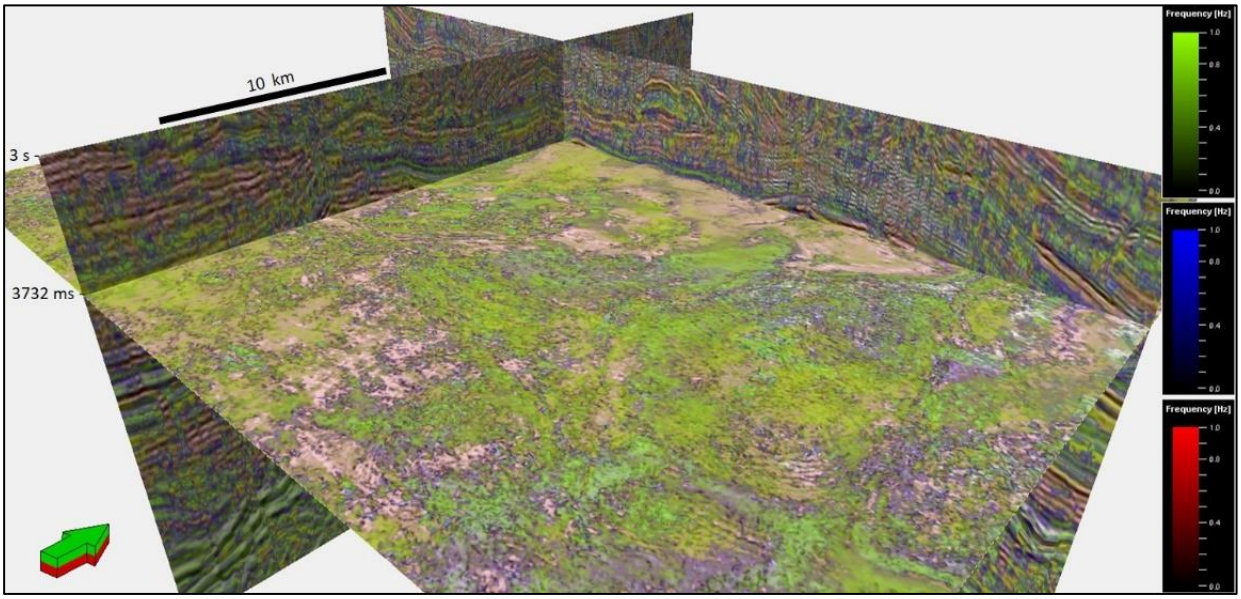

Figure 18. IsoFrequency attribute co-rendered with seismic amplitude (vertical) and coherence (time slice), for the inline 3,714, crossline 2,000, and 3,732 ms time slice intersection. The arrow points north and green is up.

3.3. Post stack seismic inversion

With the previously computed P-impedance at the well (Figure 10), two methods were evaluated to determine the best fit between initial and synthetic models. Figures 19, 20 and 21 show the comparison between these models using different parameters and methods. Two different wavelets were used to compare the fit between seismic and well data using model based and colored inversion. The first wavelet was extracted from the seismic data using the well logs to obtain amplitude and phase, before applying the model based inversion method (Figure 19). The statistical wavelet was extracted from seismic data at the well location (inline 3,714; Figure 20) using a time window from 3,500 ms to 4,200 ms and zero-phase. As wavelets change depending on the travel time through the seismic survey, the statistical wavelet was considered the best option to use in this study. This reduced the uncertainty related to the low correlation between well logs and seismic data at the reservoir depth, given the low frequency content.

The Zp column compares the original log with the initial model and the final model (blue, black and red lines in Figure 19). The initial model is the acoustic impedance considering the selected parameters and the final model corresponds to the result of the inversion over seismic data. The synthetic trace is the result of the inversion, and the error column shows the difference between the synthetic and seismic trace. In the first case, there is a high correlation (0.9956) between the synthetic and seismic trace (Figure 19), however, the initial and final models have a difference of ~2,800 m/s*g/cc (Zp column, top).

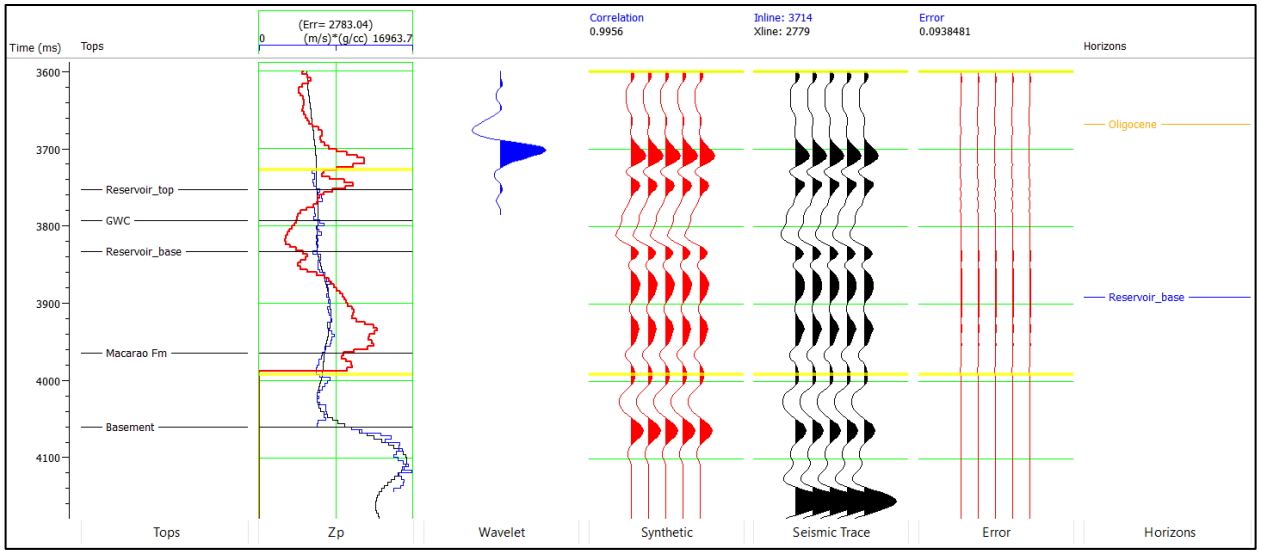

Figure 19. Inversion analysis, Orca-1 well to the Jarara 3-D seismic volume. Model based inversion method from the Geoview® suite using the Orca-1 well wavelet. The upper limit is above the reservoir top and the lower limit is inside the Macarao Formation. The Zp column shows the original log in blue, the initial model in black, and the final model in red.

The colored inversion method uses an operator (Figure 21) to consider both the spectrum from seismic amplitudes and acoustic impedance from well logs, making colored inversion a consistent method with the subsurface reflection coefficient series in the area, regarding the data available from well (Lancaster and Whitcombe, 2000). Colored inversion (Figure 22) provided an acceptable correlation number (0.74) and a small error when comparing initial and final models in terms of acoustic impedance (~1,490 m/s*g/cc). The colored inversion method provides a relative acoustic impedance visualization of the seismic data. This is applicable in this case given the low frequency of the data (15 Hz) at the reservoir depth (3,600 – 4,000 ms) and the lack of enough samples from well data to create a statistical inversion workflow.

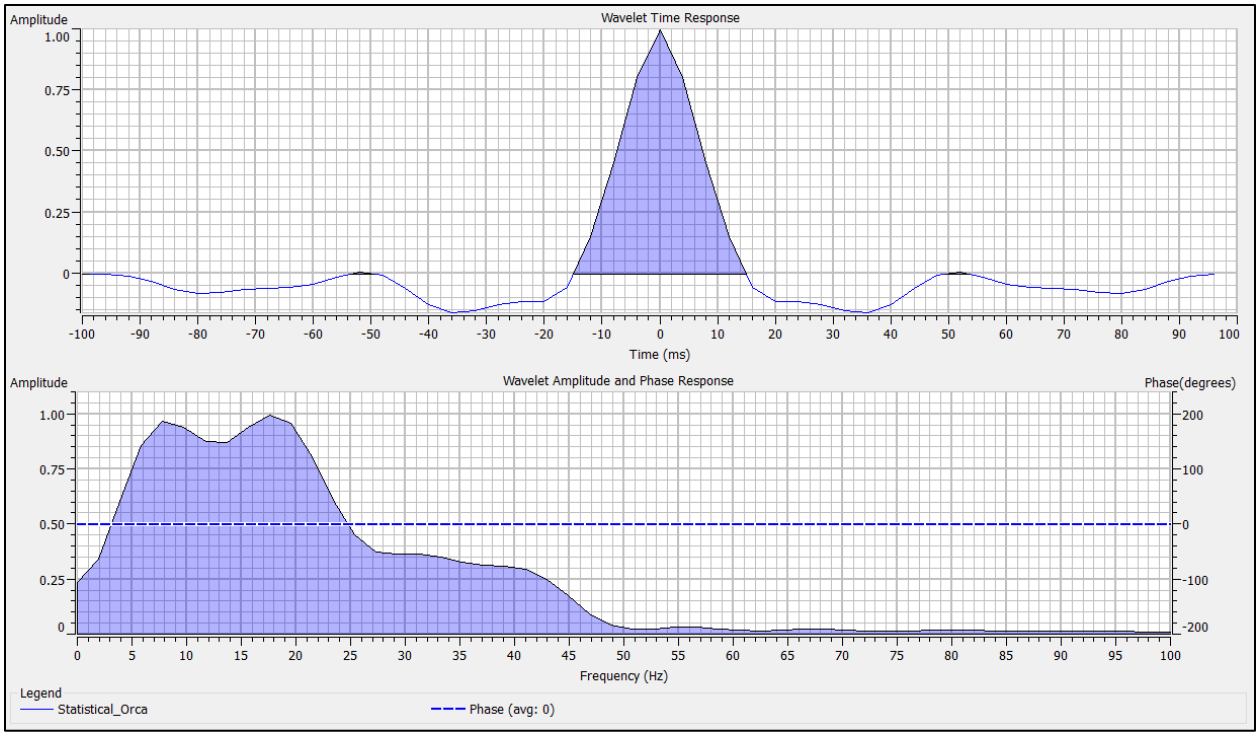

Figure 20. Statistical wavelet used for the colored inversion method from the Geoview® suite. Note amplitude spectrum and time response of the statistical wavelet at the well location (inline 3,714).

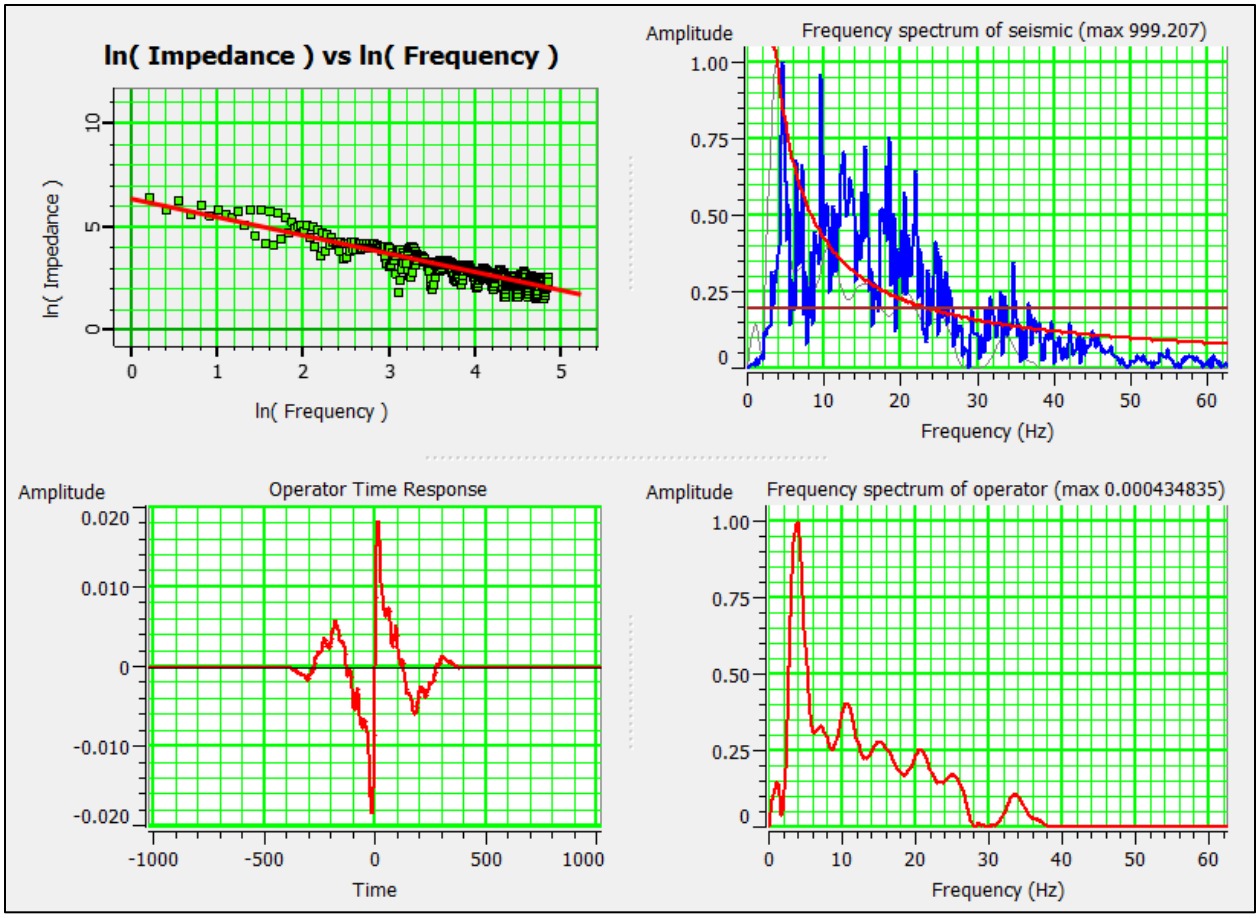

Figure 21. Inversion operator time response and frequency spectrum, colored inversion method from the Geoview® suite.

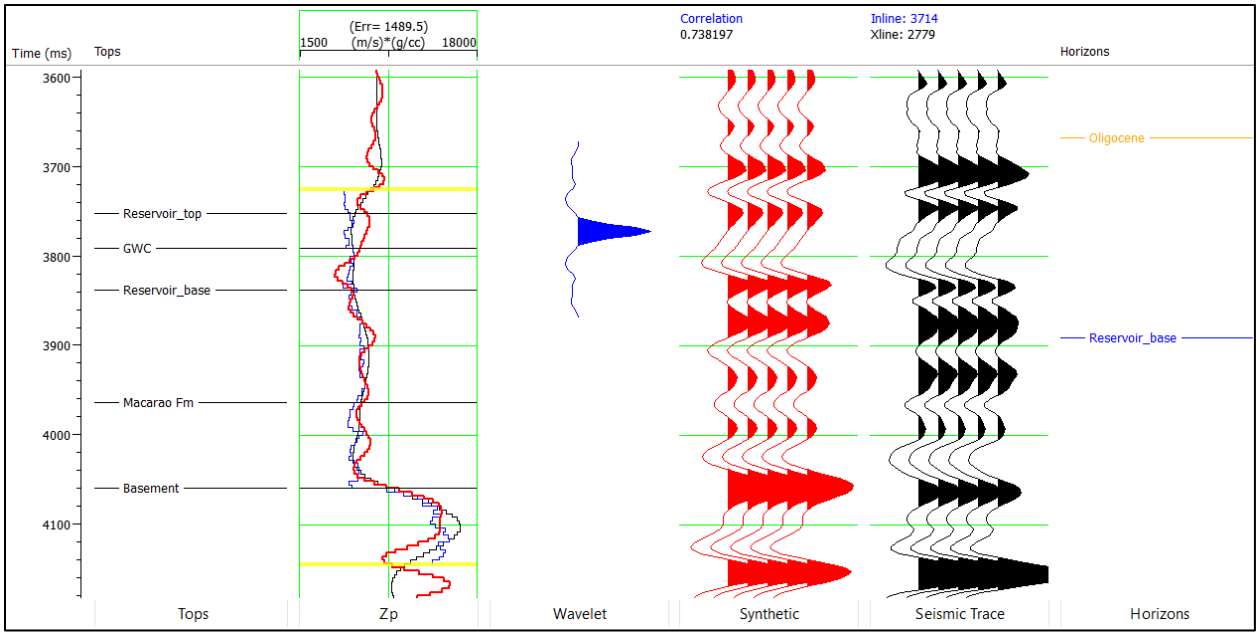

Figure 22. Inversion analysis, Orca-1 well to the Jarara 3-D seismic volume. The colored inversion method from the Geoview® suite using a statistical wavelet. The upper limit is above the reservoir top and the lower limit is inside the basement. The Zp column shows the original log in blue, the initial model in black, and the final model in red.

Quality control was achieved by applying the inversion to a single seismic section. Inline 3,714 (coincident with the well) was used to evaluate which method to use for the entire seismic volume (Figures 23 and 24). The colored inversion method was chosen given the better definition of the reservoir limits at the well location, and the good correlation (0.74) between the seismic amplitude spectrum and the acoustic impedance spectrum from the well. Figure 25 is a composite view to check the inversion results by comparing the initial model (a, view 1), the inversion result (b, view 2) and the post stack seismic data (c, view 3).

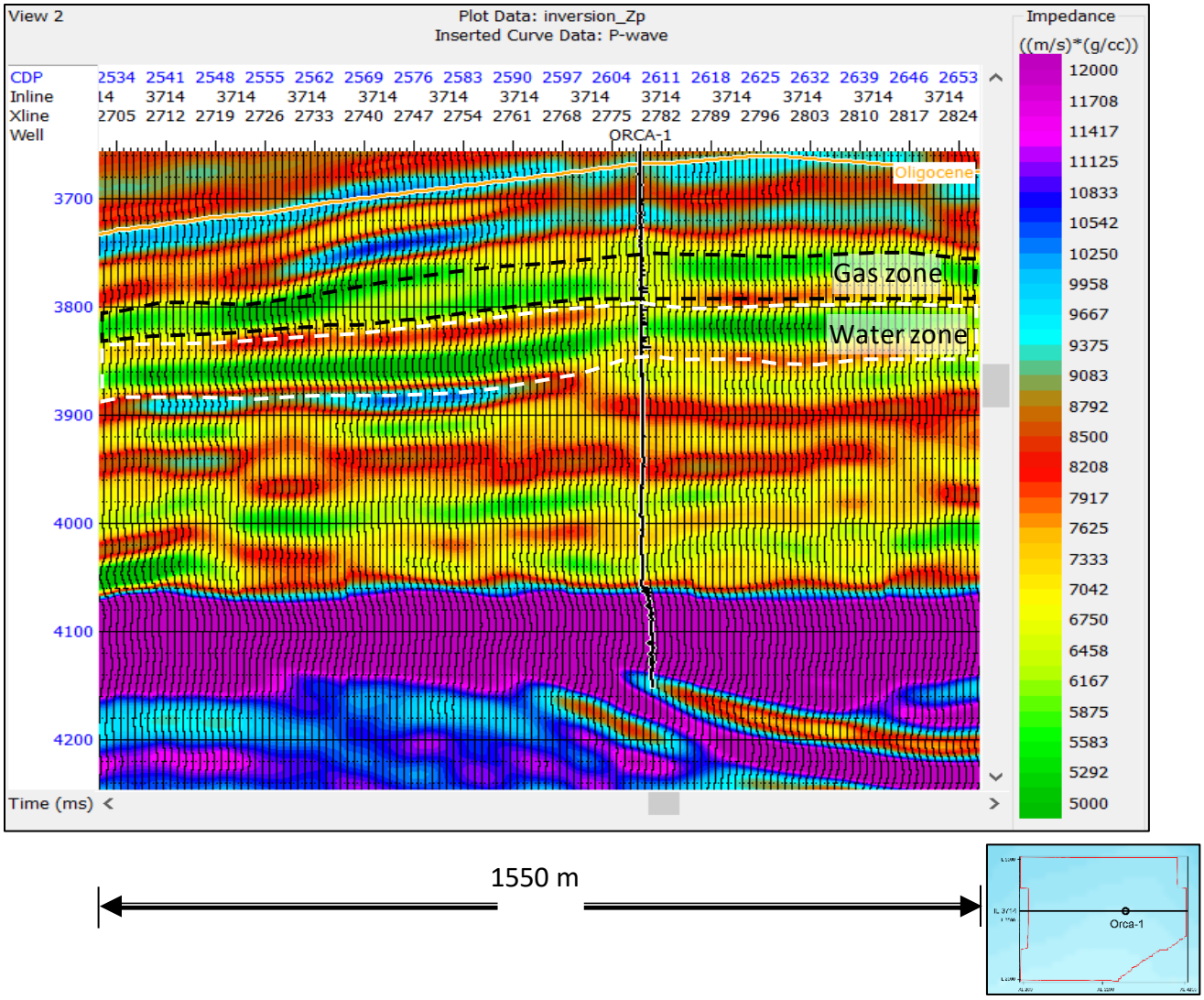

Figure 23. Inversion quality control, Orca-1 well to the Jarara 3-D seismic volume. Model based inversion method from the Geoview® suite using the Orca-1 well wavelet. The upper limit is above the reservoir top and the lower limit is inside the Macarao Formation.

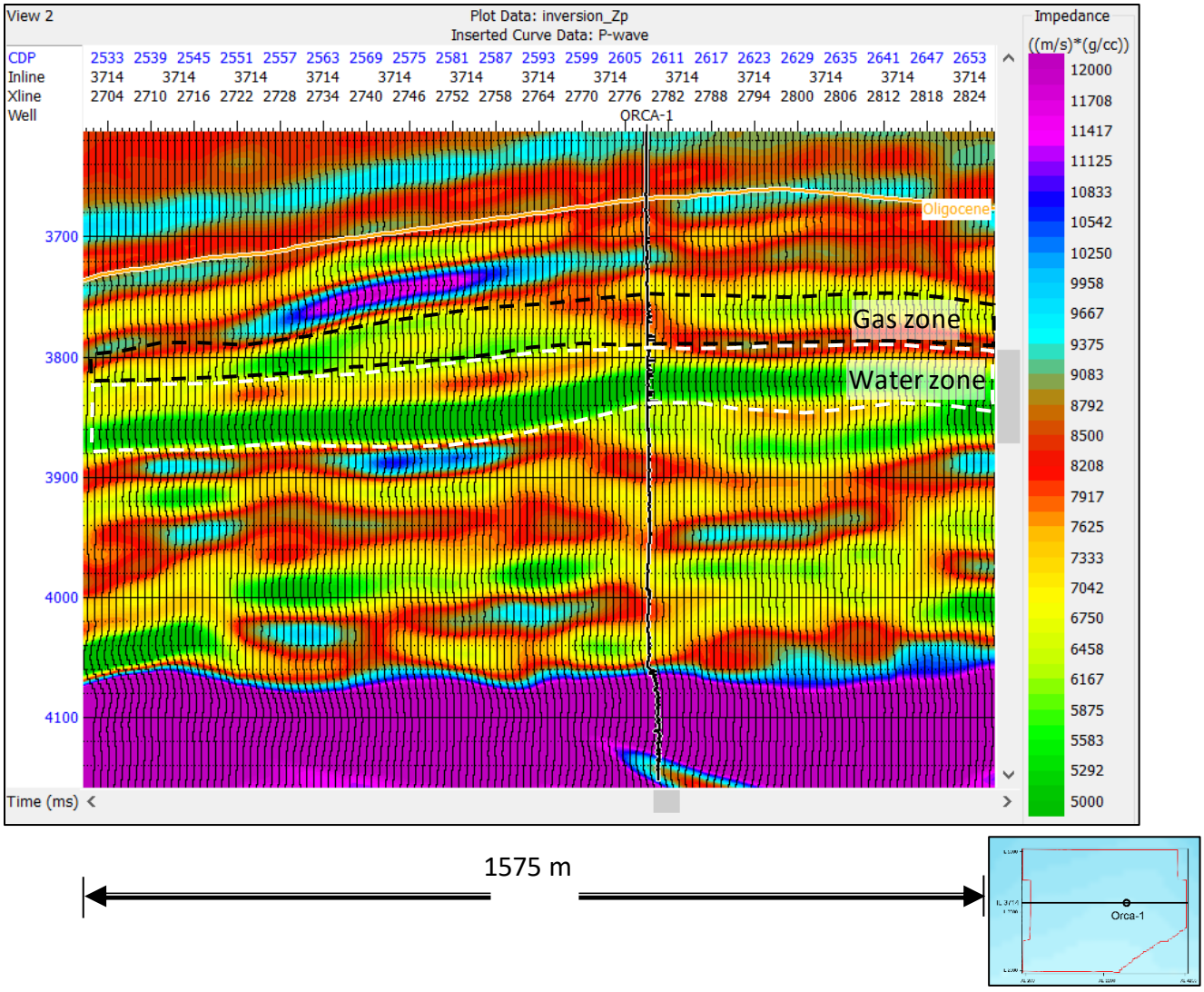

Figure 24. Inversion quality control, Orca-1 well to the Jarara 3-D seismic volume. Colored inversion method from the Geoview® suite using the statistical wavelet. The upper limit is above the reservoir top and the lower limit is inside the basement.

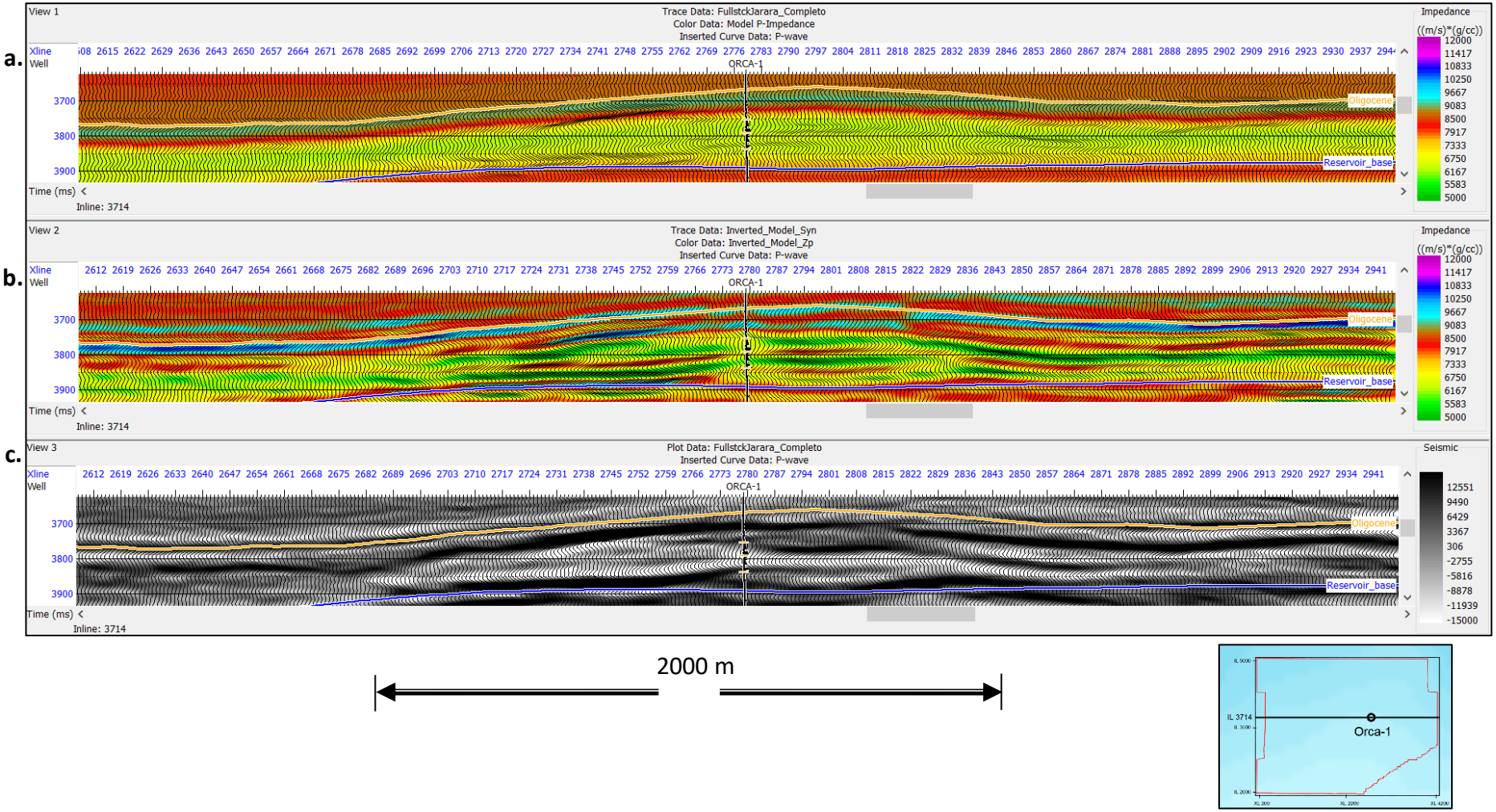

Figure 25. Composite view for inversion quality control, Orca-1 well to the Jarara 3-D seismic volume. Colored inversion method from the Geoview® suite using a statistical wavelet. The upper limit is above the reservoir top and lower limit is inside the base ment. Comparison between the initial model (a, view 1), inversion result (b, view 2) and seismic amplitude (c, view 3).

4. DISCUSSION

4.1. Well to seismic tie

The Orca-1 well was drilled over a basement high almost 10 km wide. Figure 26 shows the relative acoustic impedance section at the well location. The well reached its target at 3,583 m (MD) after drilling the whole Miocene sequence (Figure 7). The basement top is at 4,010 m (4,060 ms), In Inline 3,714 the reservoir is located between 3,750 ms and 3,840 ms. A complete set of wireline logs were run in the zone of interest (Table 2), including nuclear magnetic resonance (NMR), sidewall cores, borehole images and a modular formation dynamics tester (MDT).

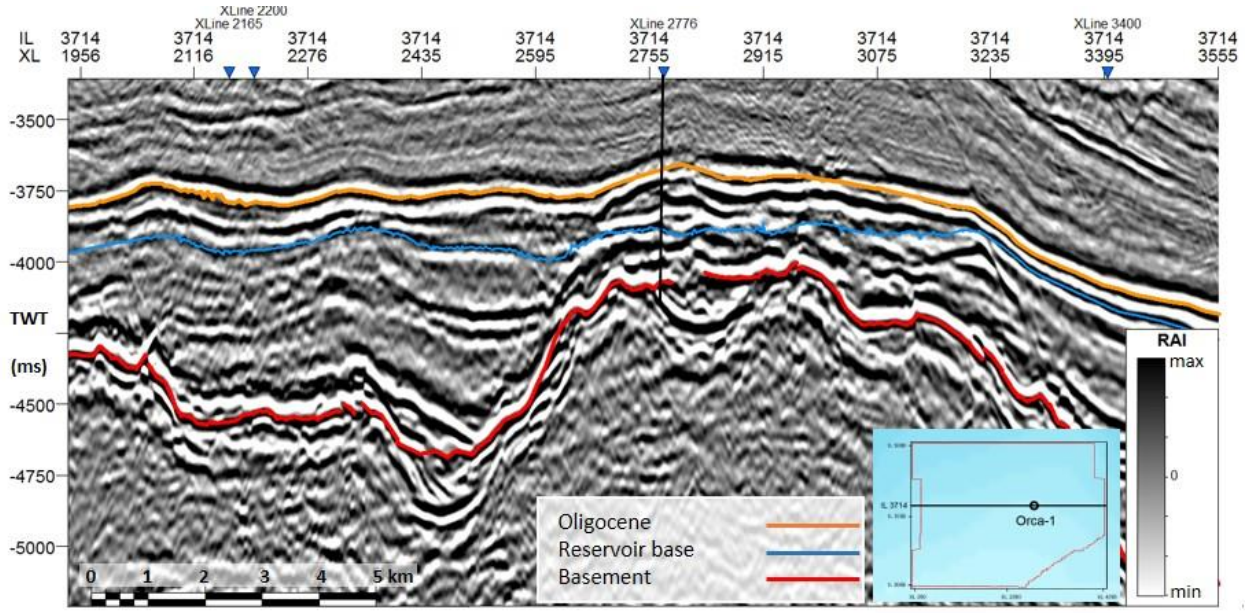

Figure 26. Inline 3,714 interpreted using the RAI volume. The black line located at the intersection with crossline 2,776 corresponds to the well path.

Interpretation of gamma ray readings for the well (Figure 27) describe an interbedded siliciclastic sequence. Given the low density of gas, the gas effect is shown by the density and neutron porosity where they display a crossover. This is a gas zone indicator on quick look evaluations (yellow shaded area on the Den-Neu track in Figure 27). Oil and water would produce a similar effect; however, the curves would be closer to each other in the presence of oil and overlapping in water zones. Resistivity values are also affected by the thickness of the layers, showing lower values of the normal trend in the presence of gas. This response is due to the bed thickness falling below the vertical resolution of the well logs.

Total and effective porosity, as well as permeability values shown by the petrophysical interpretation, are indicative of the good quality of the reservoir. With the MDT acquired in the interval 3,580 m to 3,690 m (MD), a gas water contact (GWC) was identified. The final DST (black bar on the GR track in Figure 27) performed in the interval 3,583 – 3,617 m (MD) confirmed the hydrocarbon potential in Guajira offshore basin.

Using gamma ray, density, and sonic logs, the elastic properties of the reservoir were calculated (Figures 10 and 11). The relationship between P-wave and S-wave velocities (V_P/V_s ratio) is related to the lithological type and fluid content in the formation. In the presence of clean sandstones, the values for this ratio range from 1.6 to 1.75 (Pickett, 1963). Higher V_P/V_s ratio are related to clay interbedding in the reservoir. Meanwhile the increasing gas saturation will move the ratio to lower values (Castagna et al. ,1985).

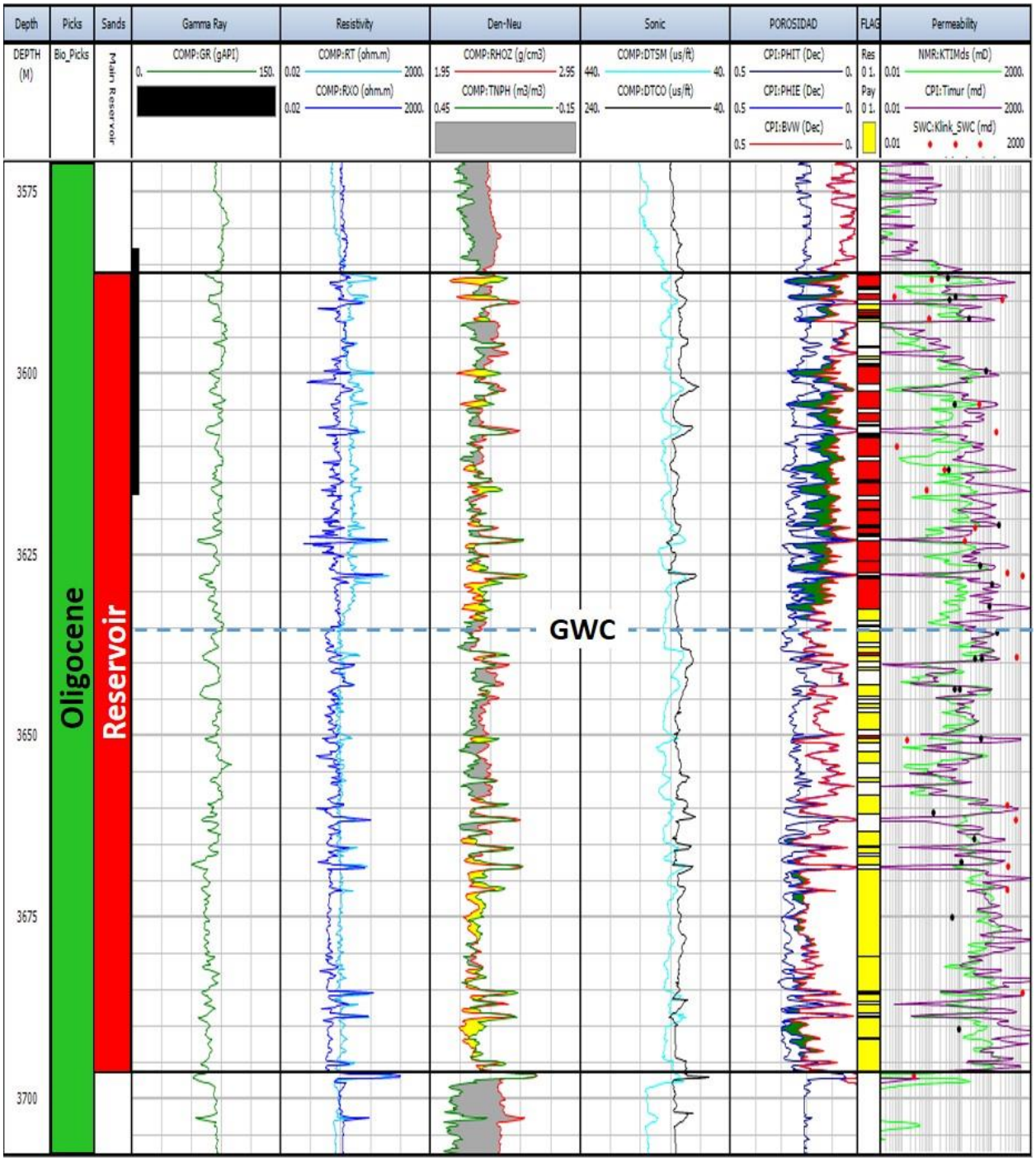

Figure 27. Reservoir petrophysical evaluation, Orca-1 well. Modified from Llinas (2015).

A visual evaluation of the V_p/V_s ratio, by comparing the curve trend inside the gas zone with the lower part of the well column, allow us to interpret that both gas and water units have reservoir potential. At least two zones in the Macarao Formation (red arrows in Figure 28) can be added to the reservoir in areas at a higher structural position. Low acoustic impedance values, which is the product of density and velocity, are used to identify the position of the gas sandstone (low density gas effect). A crossplot of the V_p/V_s ratio vs P-impedance, is used to characterize the reservoir intervals at the well (Figure 29); in this case, the red ellipse zone indicates the area where fluids and mineral content define clean sandstones with high gas saturation in siliciclastic reservoirs (Ødegaar and Avseth, 2003). Based on the V_p/V_s ratio vs P-impedance, the elastic reservoir characterization of the gas sandstone validates the quality of the water unit in terms of reservoir potential, identifies some intervals at the top of Macarao Formation with the same reservoir quality, and confirms that the analysis of the reservoir unit can be done without discriminating the gas and water zones, given the seismic resolution at this depth.

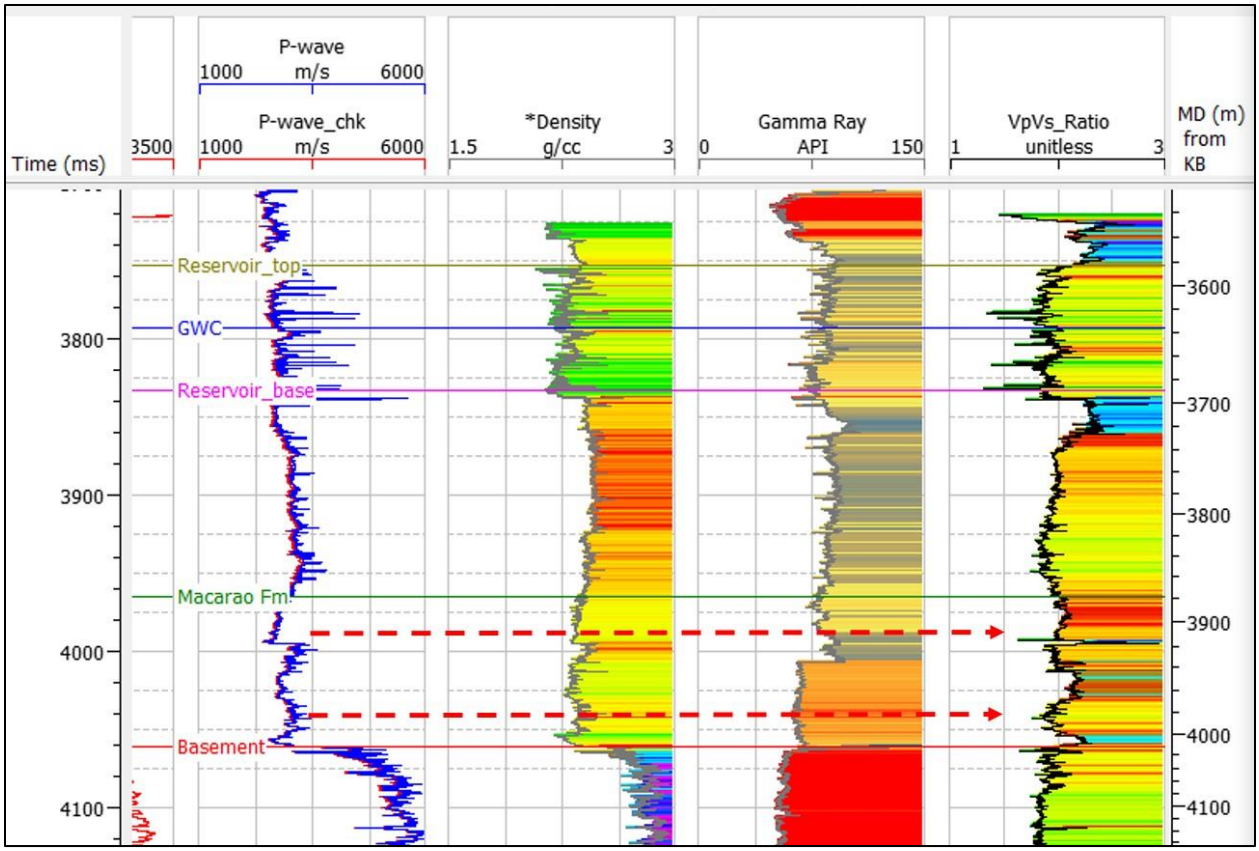

Figure 28. Elastic properties of the gas interval, Orca-1 well. Notice red dashed arrows indicating zones in Macarao Formation with reservoir potential.

4.2. Seismic attributes

The generalized stratigraphic column (Figure 4) summarizes the Tertiary sequences drilled by offshore wells in the Guajira basin and provides a correlation with onshore observations that provided a hypothetical Cretaceous source rock in the Caribbean region. As defined by Ramirez (2007), the La Luna, Macarao and Castilletes formations are the regional source rocks, meanwhile Siamana, Uitpa and Jimol formations are the reservoir units.

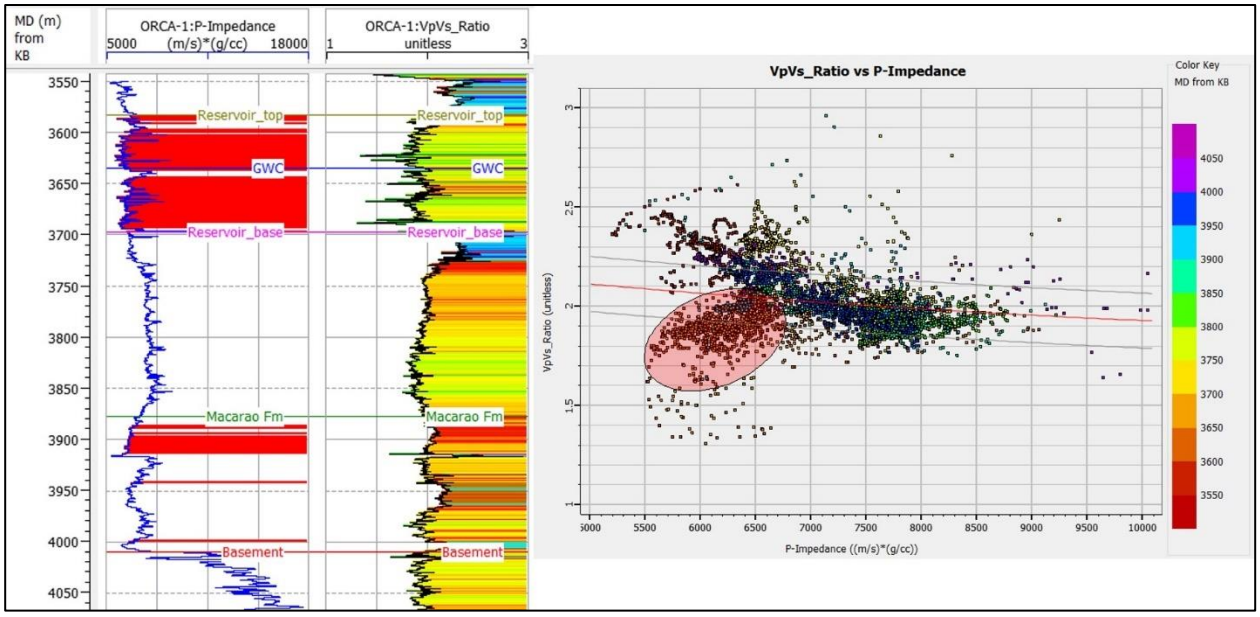

Figure 29. Elastic reservoir characterization of the interval in the Orca-1 well. A crossplot of the V_p/V_s ratio vs P-impedance is used to characterize the reservoir intervals. The red ellipse zone indicates the intervals with reservoir potential, shown in red to the right of the P-impedance log.

The depositional model indicates that Eocene and Oligocene units (Macarao and Siamana formations) were deposited intraslope, as an expression of the ponded accommodation defined by Prather in 2003 (Figure 30). For the Jarara 3-D seismic volume, the changes on the slope profile are due to volcanic rocks and basement highs related to Cretaceous syn-rift deformation (Figures 6 and 31).

A seismic section flattened along the Oligocene horizon was used to evaluate the distribution of the Eocene and Oligocene sequences. Figure 31 shows that sediment circulation was restricted by the presence of basement highs. In some areas of the basin Eocene deposits could bypass the major topographic features at that time. Considering the reservoir potential of

some intervals at the top of Macarao Formation, there is a high probability of finding good reservoir intervals in those parts of the basin where the Eocene sequence (brown shaded area) developed apron like deposits (white dotted lines) between basement highs.

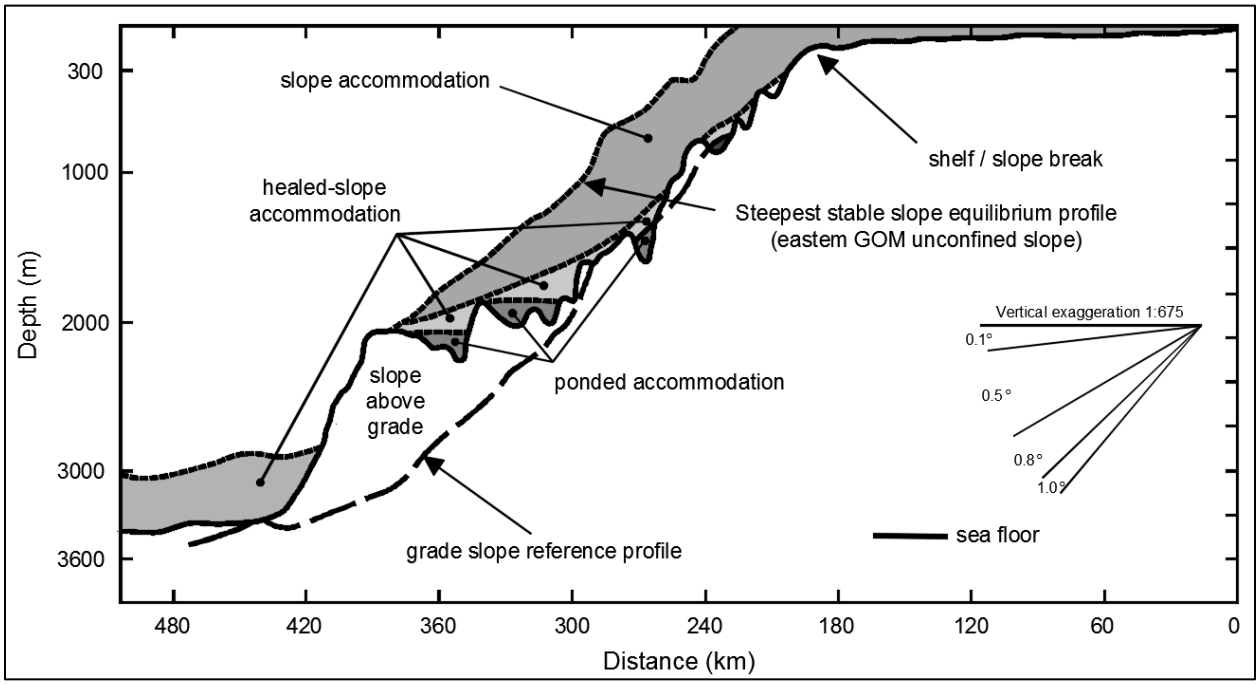

Figure 30. Sea floor profile and accommodation distribution along the slope (modified from Prather, 2003).

Based on the attribute volumes generated using Petrel's algorithms, the seismic response of the reservoir and its continuity through the study area was evaluated. Identification of stratigraphic bodies equivalent to the drilled reservoir was carried out using the acoustic impedance volume. The Oligocene and the base of the reservoir horizon have a constant

distribution and ellipsoidal geometry (Figures 32 and 33). The structural closures have a NE-SW trend in accordance with the regional trend of tectonic features developed during the Caribbean plate evolution at the northern end of South America (Figure 1e).

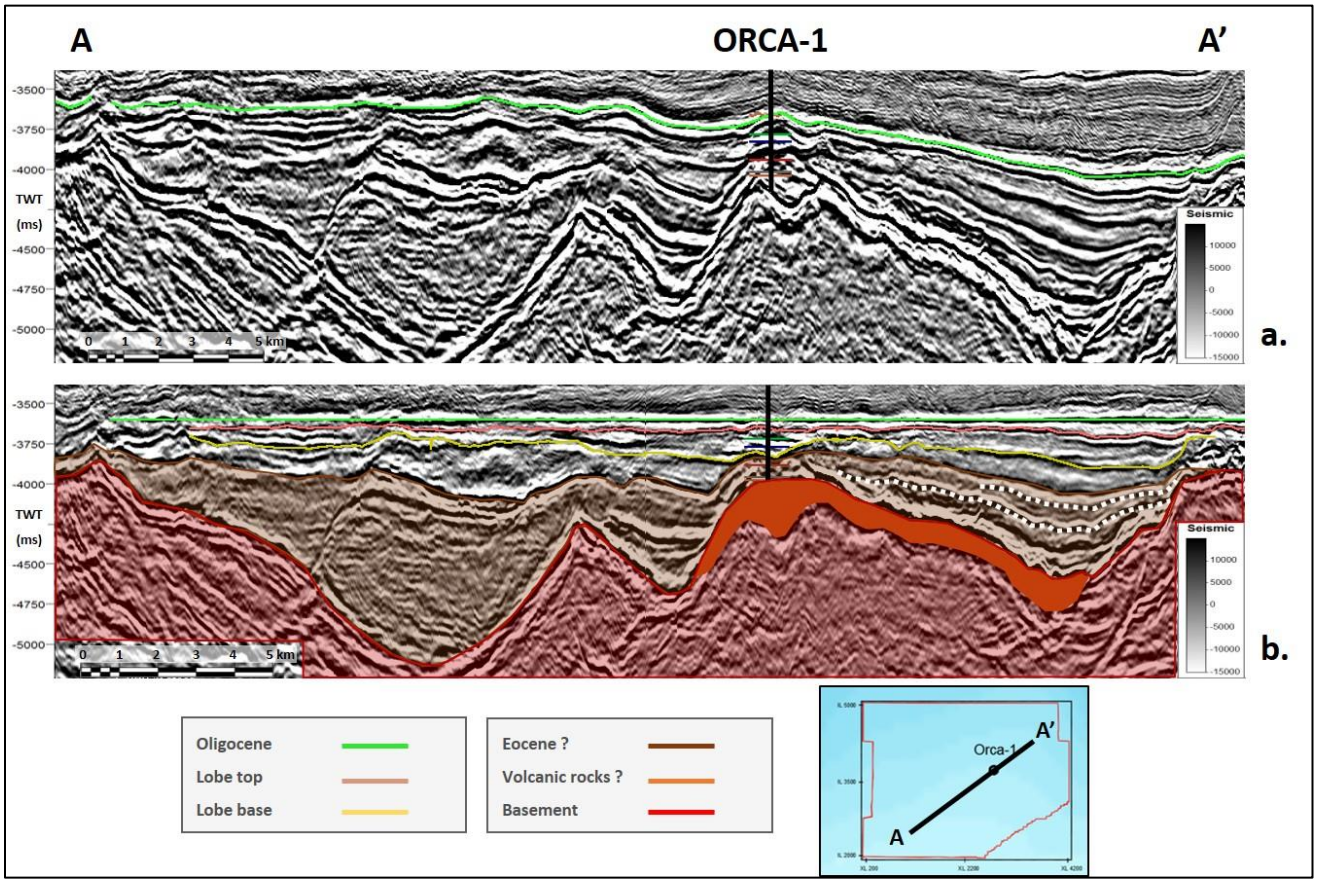

Figure 31. (a) Eocene and Oligocene sequences ponding between basement highs in the Guajira offshore basin. (b) Comparison with a flattened arbitrary seismic section using the Oligocene horizon as a datum. White dotted lines indicating the location of apron like deposits within basement highs.

The integrity of the Oligocene and Lower Miocene sequences is shown by the high coherence values through the seismic cube (Figure 14). As there are no signs of faulting or discontinuities across the sequence, it can be designated as a good seal rock.

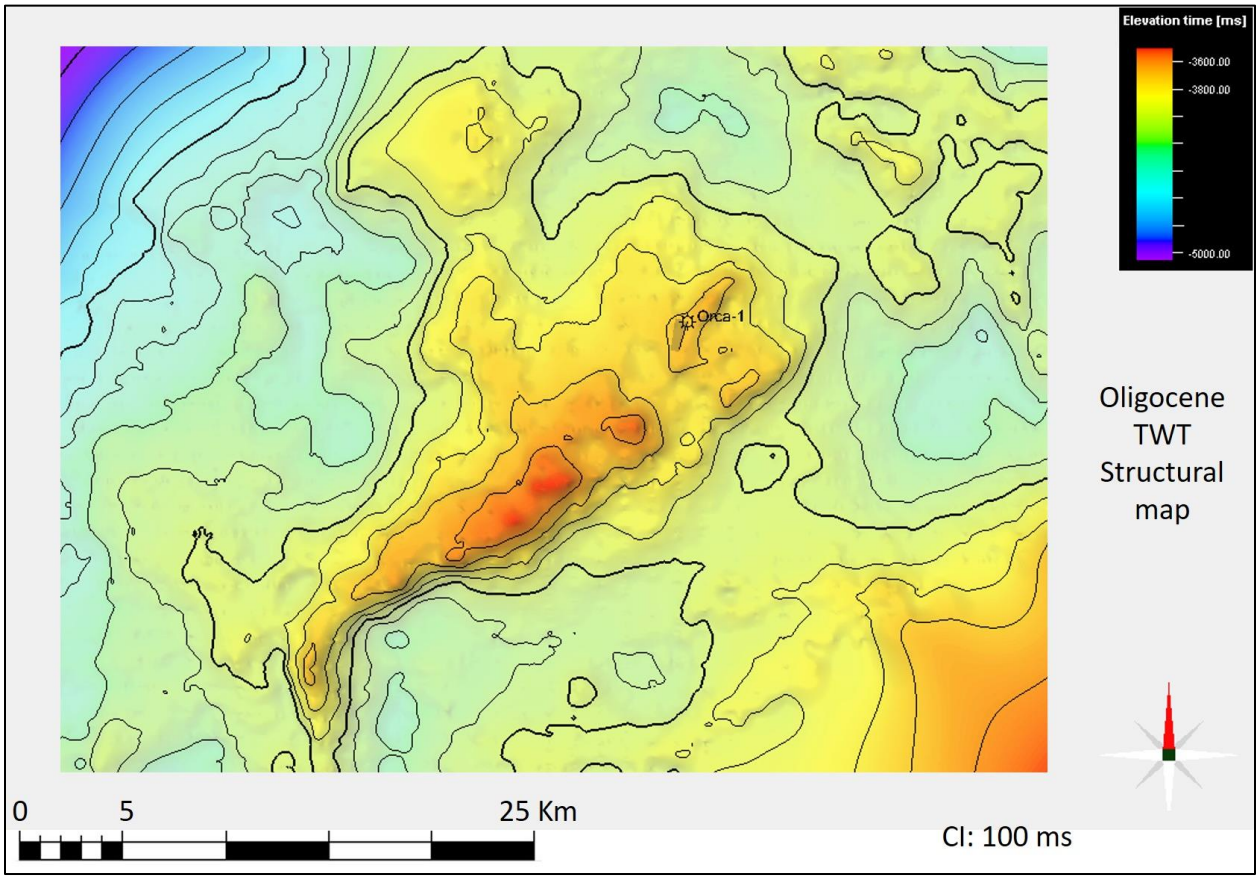

Figure 32. Structural map in TWT at the Oligocene horizon in the Jarara 3-D seismic volume.

The Upper Miocene-Pliocene angular unconformity is an expression of the deformation that occurred during the collision between the South American and Caribbean and plates in

Neogene time (Mantilla et al., 2013; Figure 6). The Oligocene and the base of the reservoir horizons are not affected by Neogene time faulting, therefore the Oligocene to Lower Miocene sequences behave as a mechanical barrier, isolating traps related to a hypothetical Eocene – Oligocene petroleum system in the Guajira offshore basin.

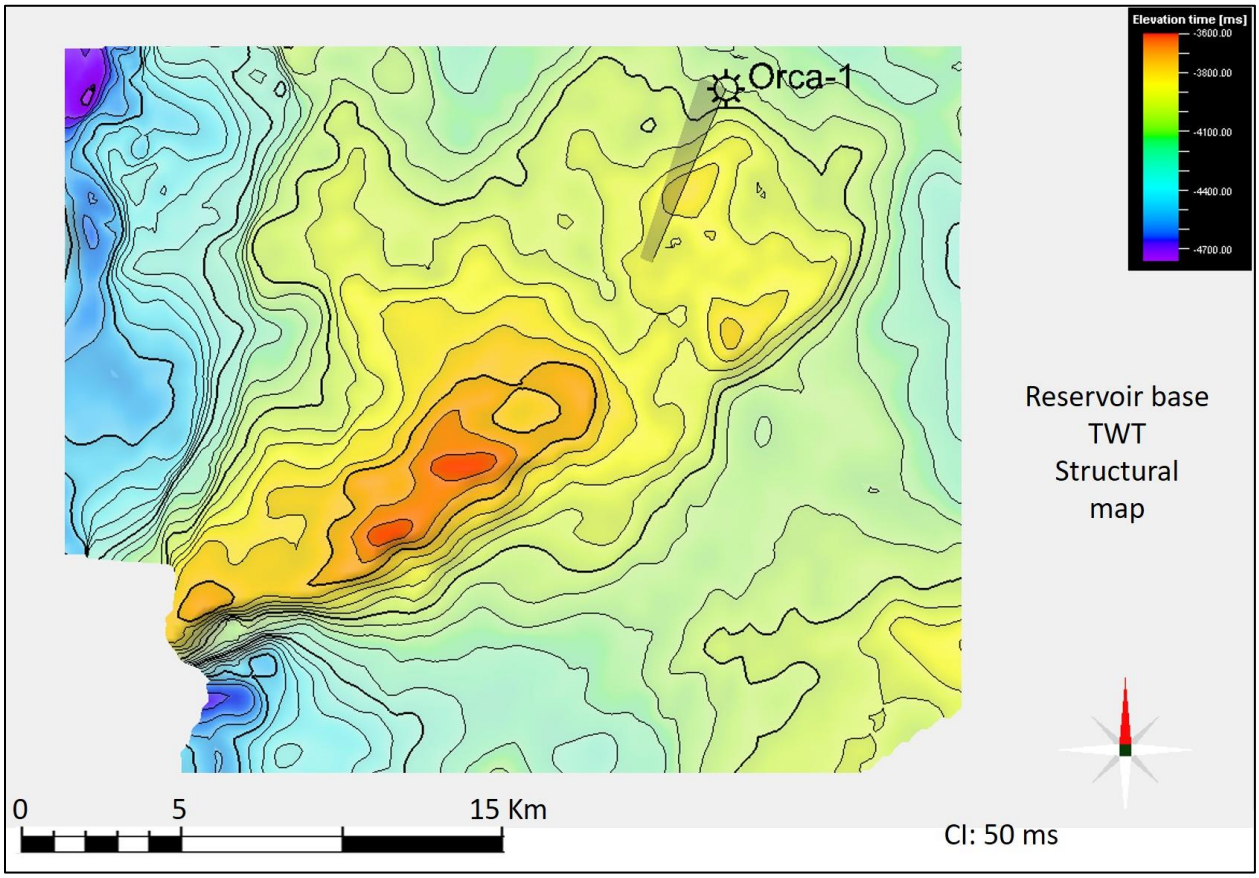

Figure 33. Structural map in TWT at the base of the reservoir in the Jarara 3-D seismic volume.

Using a multiattributes display, a visual evaluation of the attributes computed was carried out to determine the contribution of seismic attributes to reservoir identification and characterization. Figures 34 to 36 present coherence and sweetness (co-rendered in an inline – crossline – time slice display) as those attributes that helped to define the depositional model, correlate deposits, and differentiate lithologies.

The multiattributes display clearly shows channel features that can be defined at two different time slices, both related to the stratigraphic bodies drilled by the Orca-1 well. Some channelized features can be seen using coherence alone and when co-rendering coherence and sweetness. At 3,732 ms, the channelized deposits have a perpendicular distribution (EW and NS), suggesting the existence of a complex system with distributary channels operational at different times to supply the sediment to fill in the basin. The channel infill is categorized as fine-grained sedimentary rocks given the low sweetness values. This is the seal rock in this part of the basin (Figure 34).

For the 4,160 ms time slice (Figure 35), the channels are strongly controlled by the paleo-topography. At this depth, the main channel has a southeast to north west trend. The channel infill has high values of coherence and sweetness, indicating sandstone content. An image of the well location inline (Figure 36) allows differentiation of siliciclastic deposits inside the channel from the basement, which also has high sweetness values. The interpretation is that ponded accommodation was created by basement erosion. Deeper deposits in the northern part of the

Jarara 3-D volume may have a high lithic content at the base of the Eocene sequence due to basement erosion.

Petrophysical properties, integrating geostatistics and the multiattributes response from seismic data, have been estimated by different authors in development fields to predict reservoir qualities (Pearson and Hart, 2004). If a second well is drilled in the future, further interpretation can be done using the multiattributes response and applying statistical assessment (e.g., cross-plot analysis, correlation coefficients) to estimate other petrophysical properties from the seismic data (e.g., porosity, density; Pearson and Hart, 2004).

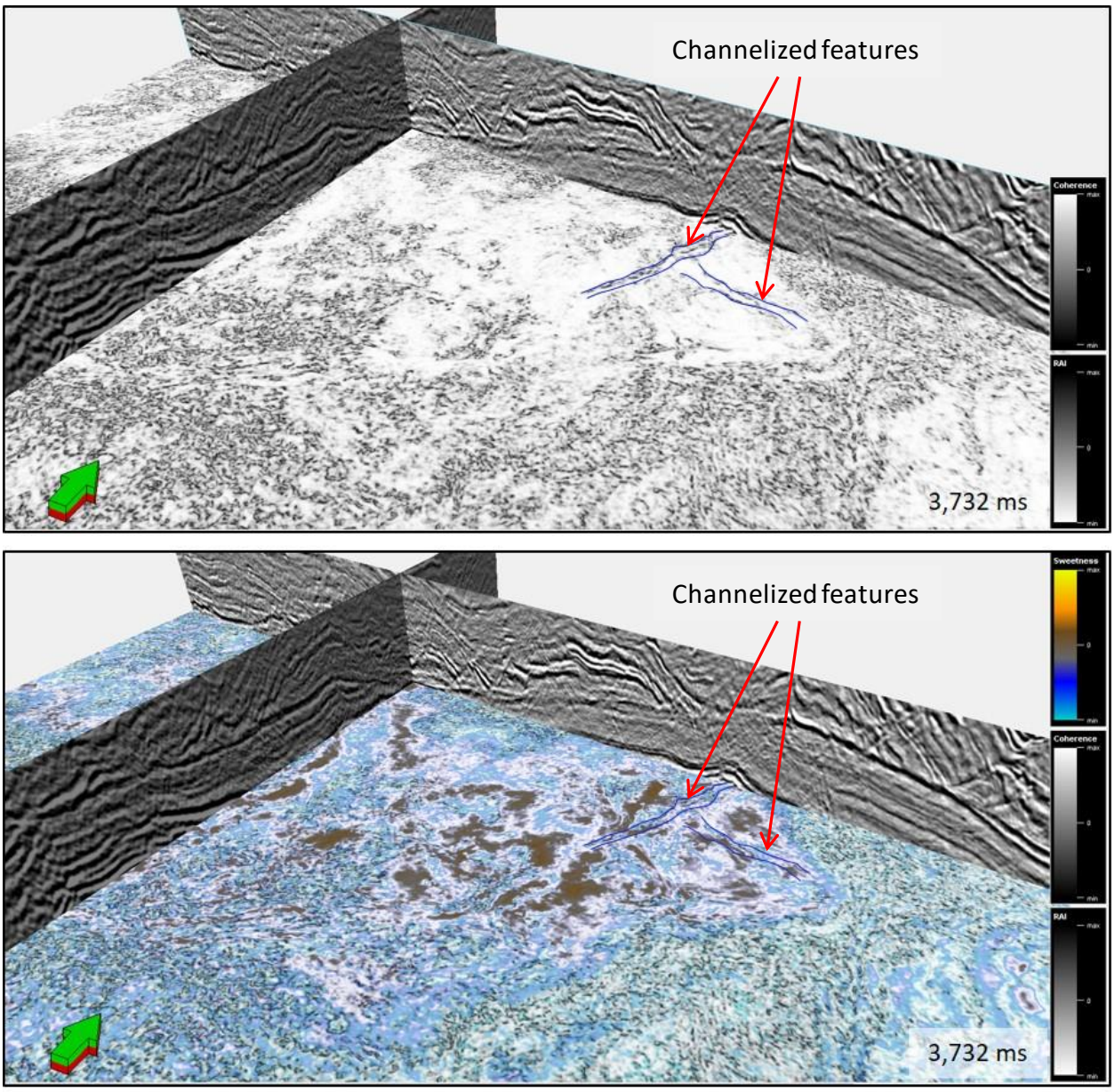

Figure 34. Coherence attribute (a and b) co-rendered with sweetness (b) in a time slice at 3,732 ms. Inline 4,000 and crossline 2,000 are shown with relative acoustic impedance (RAI). Notice the channelized features feeding the reservoir area drilled by the Orca-1 well. The arrow points north, green is up.

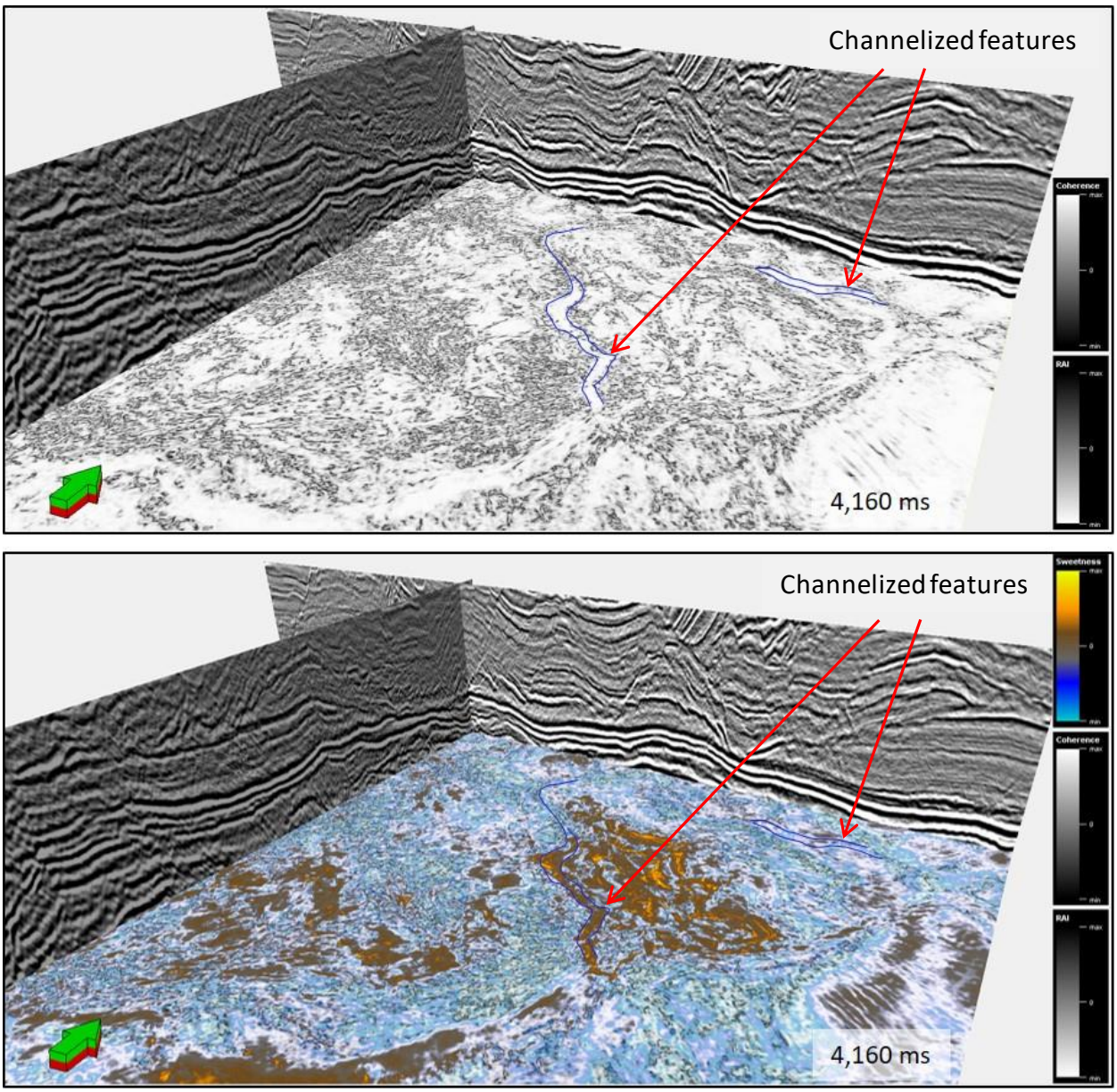

Figure 35. Coherence attribute (a and b) co-rendered with sweetness (b) in time slice at 4,160 ms. Inline 4,244 and crossline 2,000 are shown with relative acoustic impedance (RAI). Notice the channelized features feeding the reservoir area drilled by the Orca-1 well. The arrow points to north, green is up.

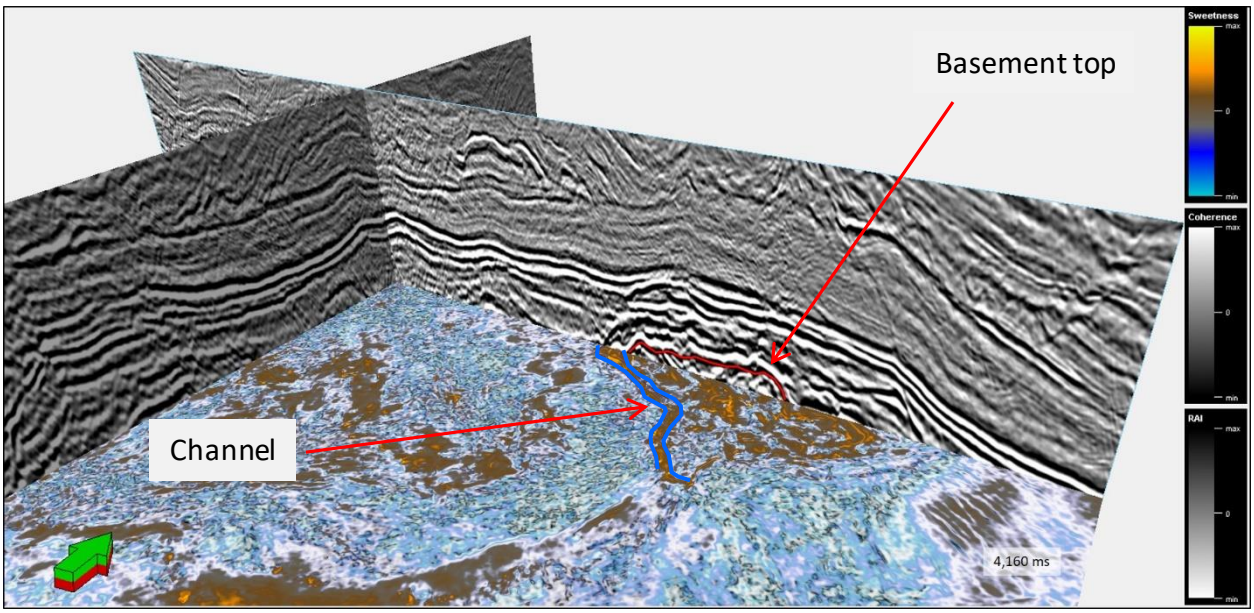

Figure 36. Coherence attribute co-rendered with sweetness in time slice at 3,732 ms. Inline 3,714 and crossline 2,000 are shown with relative acoustic impedance (RAI). Notice the channelized feature over the basement drilled by the Orca-1 well. The arrow points to north, green is up.

4.3. Post stack seismic inversion

The acoustic impedance volume obtained after post stack seismic inversion is the last attribute that can be used to define the geometry and distribution of the reservoir drilled by the Orca-1 well. As seen with the V_p/V_s ratio vs P-impedance crossplot (Figure 29), gas and water zones have the same good reservoir quality with low impedance values that range from 5,500 to 6,800 m/s*g/cc. Figures 37 and 38 summarize in a time slice view the inverted volume starting at 4,000 ms. Moving upwards in 100 ms steps through the seismic volume, the ellipsoidal structural trap can be defined, and a low impedance trend appears at the gas zone in green to yellow colors (3,750 ms – 3,840 ms), characterizing the reservoir within the structure. The final slices (Figure

38) show the area outside the model (red areas covering the structure at 3,500 ms and 3,400 ms), where the inversion was done without well control.

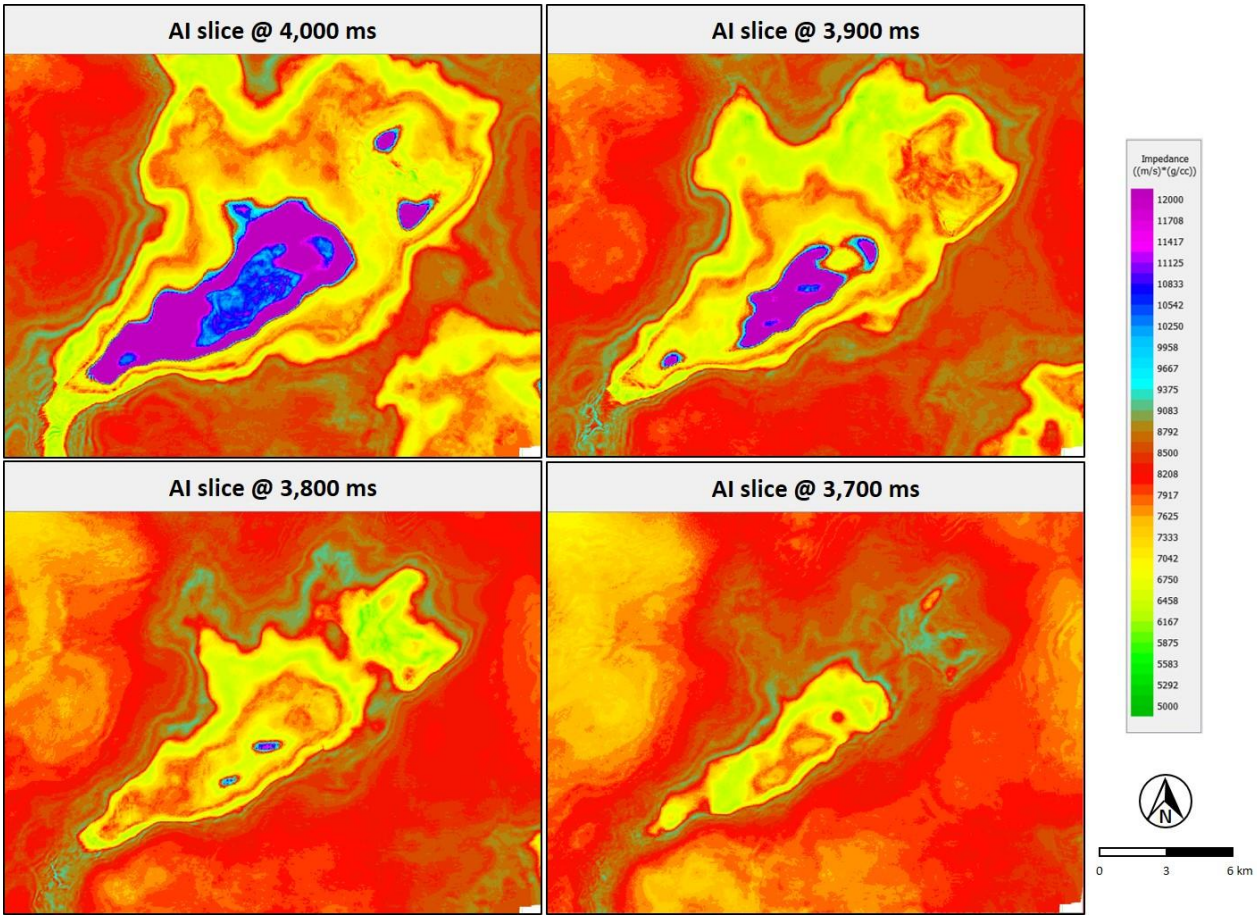

Figure 37. Acoustic impedance inversion, Orca-1 well to the Jarara 3-D seismic volume. Colored inversion method from the Geoview® suite using a statistical wavelet. The upper limit is above the reservoir top and lower limit is inside the basement. Acoustic impedance slices for 4,000 ms, 3,900 ms, 3,800 ms, and 3,700 ms.

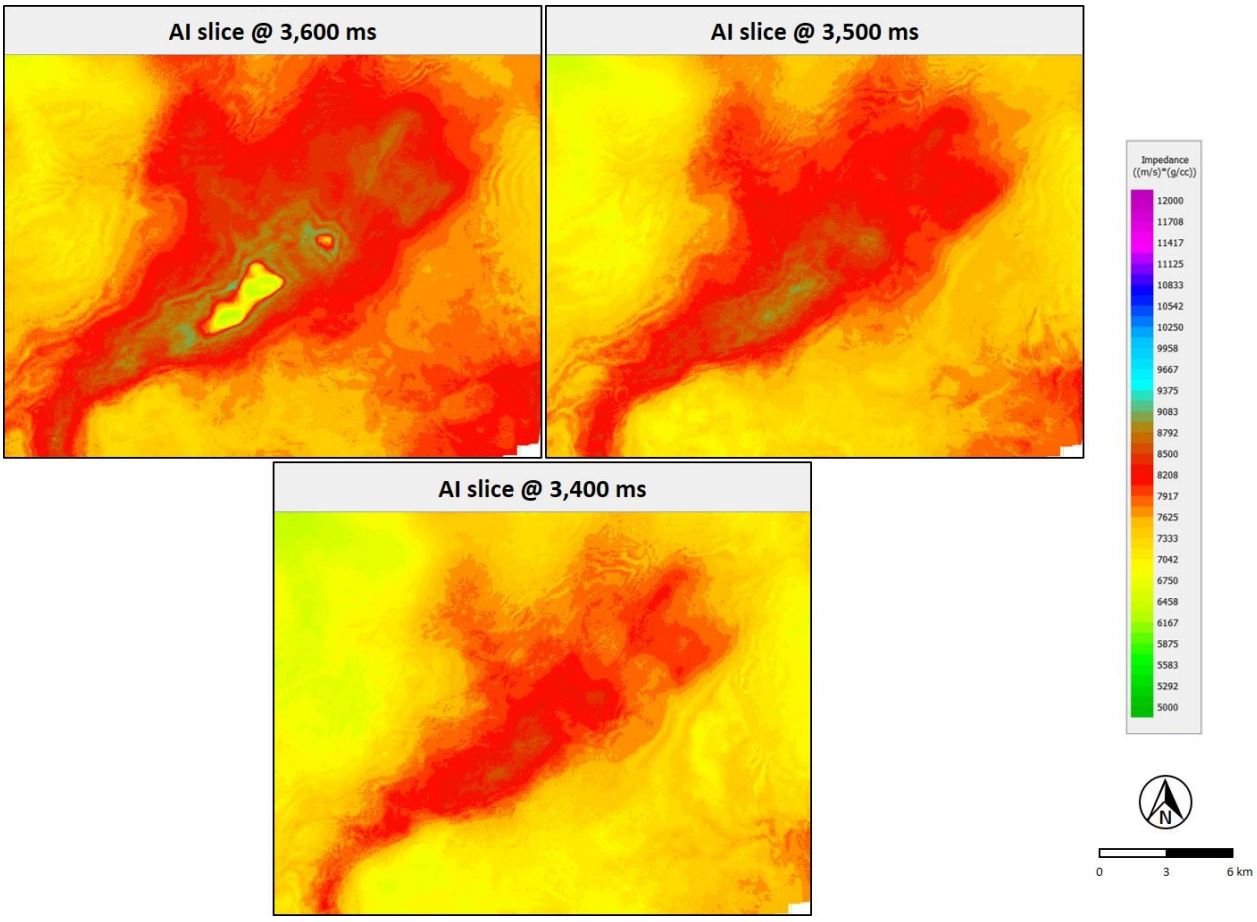

Figure 38. Acoustic impedance inversion, Orca-1 well to the Jarara 3-D seismic volume. Colored inversion method from the Geoview® suite using a statistical wavelet. The upper limit is above the reservoir top and lower limit inside the basement. Acoustic impedance slices for 3,600 ms, 3,500 ms, and 3400 ms.

5. CONCLUSIONS

The Oligocene turbidite play drilled by the Orca-1 well in 2014 corresponds to a highly-laminated reservoir deposited intra-slope as an example of what Prather (2003) called ponded accommodation. In the Jarara 3-D seismic survey, the distribution of the Eocene and Oligocene sequences was controlled by basement highs. Eocene sedimentary rocks bypassed some of the major topographic features, developing apron like deposits with reservoir potential at the top of Macarao Formation. The seismic interpretation in this study establishes the lateral continuity of the drilled reservoir inside the structural trap with a NE-SW trend consistent with the regional tectonic features developed during the Caribbean plate evolution.

The V_P/V_s ratio and acoustic impedance showed the convenience of appraising the reservoir unit without gas and water zone discrimination. The reservoir interval is characterized by:

- High values of coherence and sweetness.
- V_P/V_s ratio between 1.55 and 2.1.
- Low acoustic impedance (5,500 – 6,800 m/s*gr/cc).

Post stack seismic inversion results are consistent with the elastic reservoir characterization of the gas interval, indicating areas with comparable reservoir quality inside the interpreted structure. Reservoir geometry and distribution were mapped and the reservoir

acoustic impedance, extended beyond the well into the Jarara 3-D seismic volume, defined the structural trap with a low impedance trend in the gas and water zones. This confirmed the high reservoir quality of this unit (3,750 ms – 3,840 ms).

The reservoir characterization developed in this study followed a workflow that can be an effective and convenient tool to reduce the time taken for reservoir modeling. Post stack colored seismic inversion is a practical method that should be considered a best practice in the exploration process; not only because it can be performed fast, but also because it establishes a base case that considers both the spectrum from seismic amplitudes and acoustic impedance from well logs.

Beyond this study, with at least two wells in the area, geobody extraction involving petrophysical properties, such as density and thickness porosity, could be carried out by finding the correlation between that property and multiattributes response. The proposed workflow is illustrated in Figure 39.

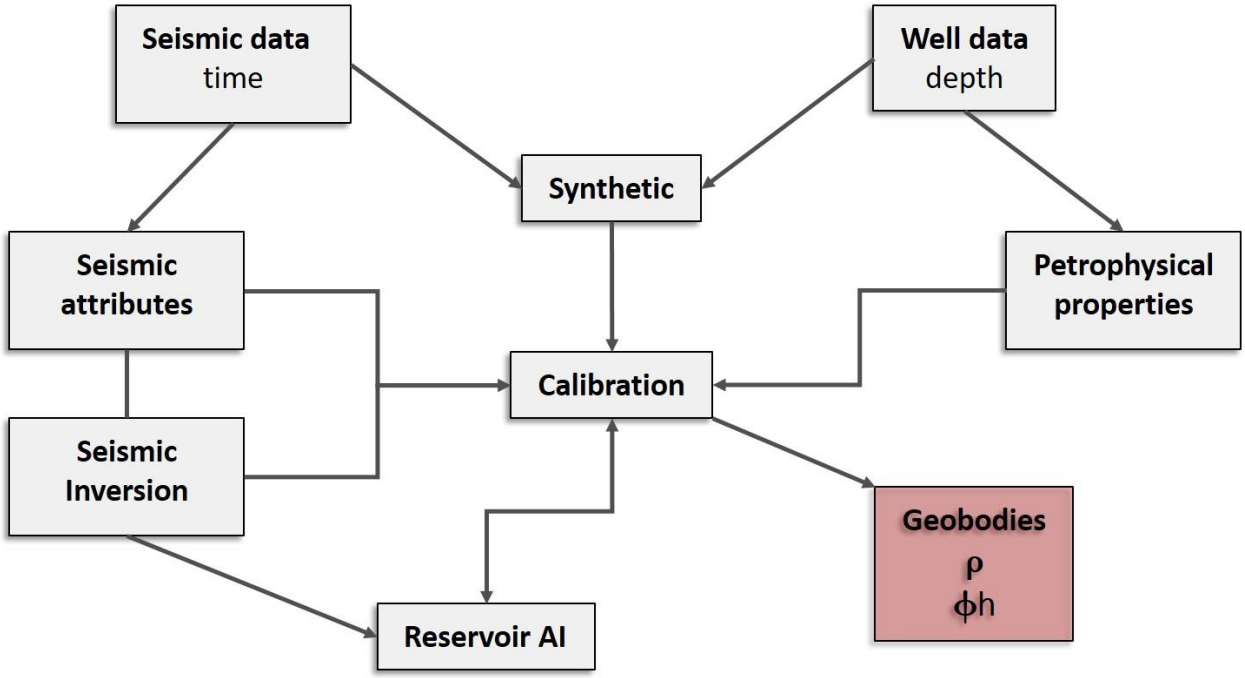

Figure 39. Workflow for reservoir characterization using post stack seismic attributes and inversion. Last step (geobody generation) can be applied when the area has two or more drilled wells (geostatistical approach). This last step is beyond the scope of this project.

REFERENCES

Bacon, M., R. Simm, and T. Redshaw, 2007, 3-D Seismic interpretation: New York, Cambridge University Press, 234 p.

Bianco, E., 2011, I is for integrated trace, http://agilescientific.com/blog/2011/12/28/i-is-for-integrated-trace.html (accessed February 26, 2016).

Castagna, J., M. Batzle, and R. Eastwood, 1985, Relationships between compressional-wave and shear-wave velocities in clastic silicate rocks: Geophysics, v. 50, no. 4, p. 571 – 581.

Cardona, A., U. Cordani, and W. McDonald, 2006, Tectonic correlations of pre-Mesozoic crust from the northern termination of the Colombian Andes, Caribbean region: Journal of South American Earth Sciences, v. 21, p. 337–354.

Ceron, J., 2008, Crustal structure of the Colombian Caribbean Basin and margins, PhD thesis, University of South Carolina, Columbia, South Carolina, 165 p.

Chopra, S., and K. Marfurt, 2007, Seismic attributes for prospect identification and reservoir characterization: Tulsa, SEG geophysical developments series, no. 11, 464 p.

De Porta, J., 1974, Lexique Stratigraphique International, Colombie, (deuxieme partie), Tertiaire et Quaternaire, Union Internationale des Sciences Geologiques: Paris, Centre Nationale de la Recherche Scientifique, 618 p.

Hart, B., 2008, Channel detection in 3-D seismic data using sweetness: AAPG bulletin, v. 92, no. 6, p. 733-742.

Lancaster, S., and D. Whitcombe, 2000, Fast track 'coloured' inversion: SEG, 70th Annual International Meeting, expanded abstracts, p. 1572 – 1575.

Llinas, J., 2015., Petrophysical interpretation of Orca-1 well: Unpublished Internal report, Ecopetrol S.A., Bogotá, Colombia.

Mantilla, O., J. Castellanos, V. Ramirez, and C. Rubio, 2013, Tectono – stratigraphic events of the northern Caribbean offshore, Colombia: International Conference and Exhibition: Cartagena, Colombia, AAPG ICE.

Ødegaard, E., and P. Avseth, 2003, Interpretation of elastic inversion results using rock physics templates: EAGE, 65th Conference and Exhibition, extended abstracts.

Pearson, R., and B. Hart, 2004, Three dimensional seismic attributes help define controls on reservoir development: Case study from the Red River Formation, Williston Basin, in Seismic imaging of carbonate reservoirs and systems: AAPG Memoir 81, p. 43 – 57.

Petrobras, Ecopetrol and Repsol, 2012, Joint Operating Agreement, Tayrona E&E Block, Technical Committee Meeting No. 01-12, recommendations to the Operational Committee Meeting: Unpublished Internal report, Petrobras International Braspetro B.V., Bogotá, Colombia.

Petrobras, 2015, Final geologic report of Orca-1 well: Unpublished Internal report, Petrobras International Braspetro B.V., Bogotá, Colombia, 73 p.

Pickett, G., 1963, Acoustic character logs and their applications in formation evaluation: Journal of Petroleum Technology, v. 15, p. 650–667.

Pindell, J., and L. Kennan, 2009, Tectonic evolution of the Gulf of Mexico Caribbean and northern South America in the mantle reference frame: an update: The geology and evolution of the region between North and South America, GSL Special Publication, v. 328, p. 1-55.

Prather, B., 2003, Controls on reservoir distribution, architecture and stratigraphic trapping in slope settings: Marine and Petroleum Geology, Elsevier, v. 20, p. 529 – 545.

Ramirez, V., 2007, Stratigraphic framework and petroleum systems modeling - Guajira Basin, offshore northern Colombia, Master's thesis, The University of Alabama, Tuscaloosa, Alabama, 169 p.

Renz, O., 1960, Geología de la parte sureste de la Península de la Guajira (República de Colombia): III Congreso Geológico Venezolano, p. 317–347.

Rollins, J., 1965, Stratigraphy and structure of the Guajira Peninsula, northwestern Venezuela and northeastern Colombia: University of Nebraska Studies, new series no. 30, 102 p.

Rubio, C., A. Hurtado, O. Mantilla, J. Castellanos, L. Vargas, and H. Niño, 2012., Folleto Geológico y Geofísico prospecto Orca-1: Unpublished Internal report, Ecopetrol S.A., Bogotá, Colombia.